Geol. Mag. **147** (*4*), *2010, pp. 611–637.* © *Cambridge University Press 2009*
doi:10.1017/S0016756809990719

Tectonic significance of synextensional ductile shear zones within the Early Miocene Alaçamdağ granites, northwestern Turkey

FUAT ERKÜL*

Akdeniz Üniversitesi, Teknik Bilimler Meslek Yüksekokulu, Dumlupınar Bulvarı, TR–07058 Antalya, Turkey

(*Received* 11 May 2009; *accepted* 25 August 2009; First published online 4 December 2009)

Abstract – Synextensional granitoids may have significant structural features leading to the understanding of the evolution of extended orogenic belts. One of the highly extended regions, the Aegean region, includes a number of metamorphic core complexes and synextensional granitoids that developed following the Alpine collisional events. The Alaçamdağ area in northwestern Turkey is one of the key areas where Miocene granites crop out along the boundary of various tectonic units. Structural data from the Early Miocene Alaçamdağ granites demonstrated two different deformation patterns that may provide insights into the development of granitic intrusions and metamorphic core complexes. (1) Steeply dipping ductile shear zones caused emplacement of syn-tectonic granite stocks; they include kinematic indicators of a sinistral top-to-the-SW displacement. This zone has also juxtaposed the İzmir–Ankara Zone and the Menderes Massif in the west and east, respectively. (2) Gently dipping ductile shear zones have developed within the granitic stocks that intruded the schists of the Menderes Massif on the structurally lower parts. Kinematic data from the foliated granites indicate a top-to-the-NE displacement, which can be correlated with the direction of the hanging-wall movement documented from the Simav and Kazdağ metamorphic core complexes. The gently dipping shear zones indicate the presence of a detachment fault between the Menderes Massif and the structurally overlying İzmir–Ankara Zone. Mesoscopic- to map-scale folds in the shallow-dipping shear zones of the Alaçamdağ area were interpreted to have been caused by coupling between NE–SW stretching and the accompanying NW–SE shortening of ductilely deformed crust during Early Miocene times. One of the NE-trending shear zones fed by granitic magmas was interpreted to form the northeastern part of a sinistral wrench corridor which caused differential stretching between the Cycladic and the Menderes massifs. This crustal-scale wrench corridor, the İzmir–Balıkesir transfer zone, may have controlled the asymmetrical and symmetrical extensions in the orogenic domains. The combination of the retreat of the Aegean subduction zone and the lateral slab segmentation leading to the sinistral oblique-slip tearing within the Eurasian upper plate appears to be a plausible mechanism for the development of such extensive NE-trending shear zones in the Aegean region.

Keywords: metamorphic core complex, synextensional granitoids, transfer zone, exhumation, crystal-plastic processes, Aegean subduction.

1. Introduction

Highly extending crustal terrains are commonly associated with the extensional detachment faults/ductile–brittle shear zones and synextensional granitoids in the immediate footwall and they are regarded as typical elements in the development of metamorphic core complexes (e.g. Lee & Lister, 1992; Lister & Baldwin, 1993; Foster & Fanning, 1997; Foster *et al.* 2001). It is now agreed that the crustal-scale extension is active during the emplacement of granitoids into the footwall extensional shear zone, but it is not yet understood if extension precedes magmatism or the magmatism causes the initiation of detachment faulting. Synextensional granitoids therefore have important structural elements which may lead to better understanding of the evolution of extended orogenic belts.

The Aegean region, one of these highly extended regions, includes a number of metamorphic core complexes that developed subsequent to the Alpine collisional event(s) (Fig. 1). Published work in the Aegean demonstrates the close spatial and temporal relationship among development of extensional detachment faults, ductile shear zones and granite emplacement (Verge, 1993; Bozkurt & Park, 1994; Hetzel *et al.* 1995*a*,*b*; Avigad, Baer & Heimann, 1998; Forster & Lister, 1999; Koçyiğit, Yusufoğlu & Bozkurt, 1999; Okay & Satır, 2000; Işık & Tekeli, 2001; Sözbilir, 2001, 2002; Pe-Piper, Piper & Matarangas, 2002; Bozkurt & Sözbilir, 2004; Işık, Tekeli & Seyitoğlu, 2004; Ring & Collins, 2005; Thomson & Ring, 2006).

Granitoids in western Turkey are thought to have been emplaced passively along NE-trending strike-slip shear zones (Kaya *et al.* 2007) or in the footwall of the extensional detachment faults (Hetzel *et al.* 1995*a*,*b*; Okay & Satır, 2000; Bozkurt, 2004; Işık, Tekeli & Seyitoğlu, 2004; Beccaletto *et al.* 2005; Ring & Collins, 2005; Thomson & Ring, 2006; Glodny & Hetzel, 2007). Emplacement of the granitoids in the Aegean region is attributed to the crustal-scale horizontal extension and consequent ductile and brittle

*Author for correspondence: fuaterkul@akdeniz.edu.tr

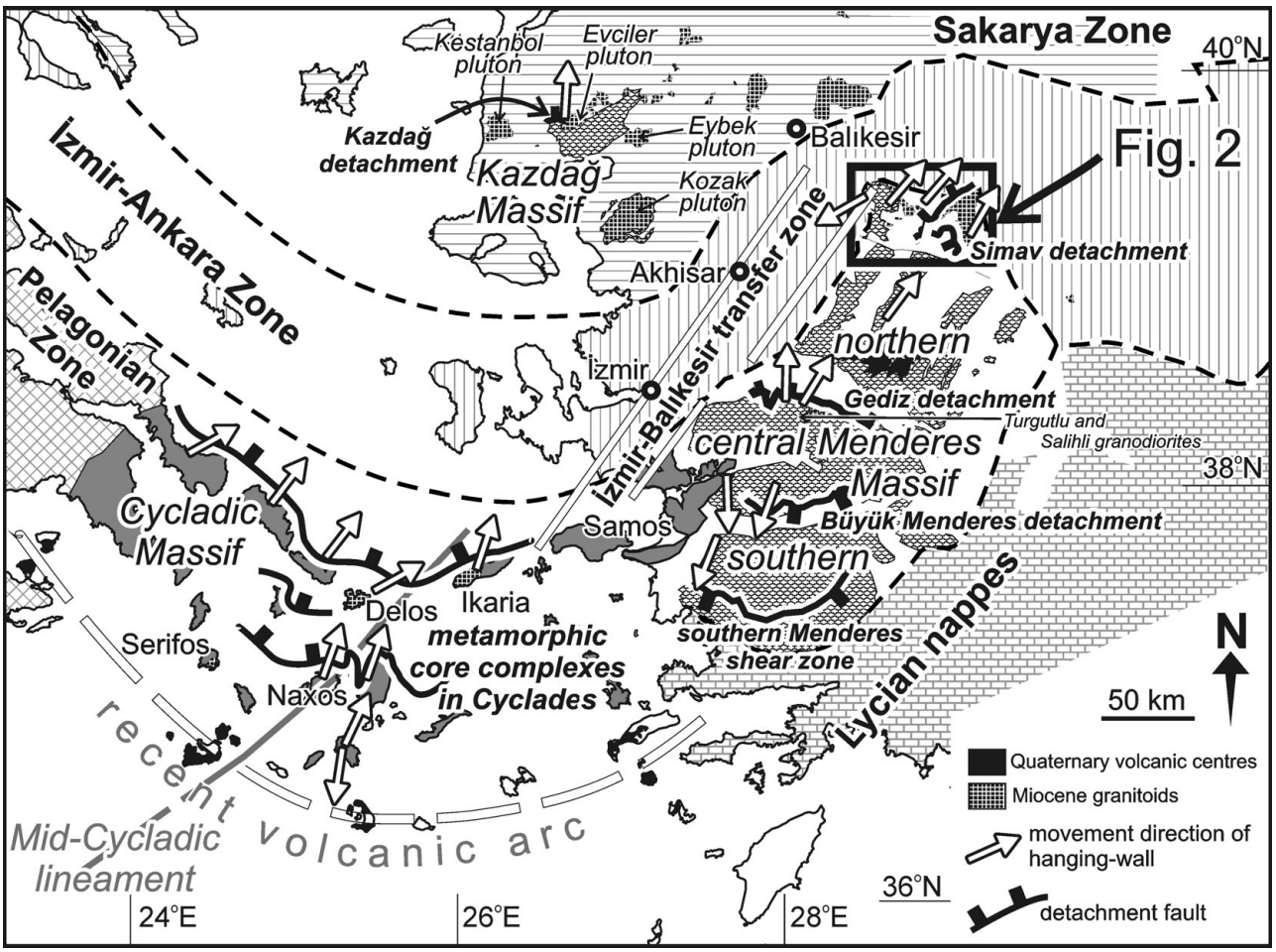

Figure 1. Tectonic map of the Aegean region showing tectonic units, major tectonic structures, metamorphic massifs, syntectonic granitoids and Neogene extension directions (structural data are from Lee & Lister, 1992; Hetzel *et al.* 1995*b*; Walcott & White, 1998; Bozkurt & Satır, 2000; Okay & Satır, 2000; Işık & Tekeli, 2001; Jolivet *et al.* 2004; Ring & Collins, 2005).

deformation that commenced by Latest Oligocene–Early Miocene times (Jolivet & Brun, in press and references therein). However, some researchers proposed that the post-collisional compressional events following the Neotethyan collisional events continued until the end of Middle Miocene times (Altunkaynak & Yılmaz, 1998; Genç, 1998; Karacık & Yılmaz, 1998; Westaway, 2006). Therefore, the origin and tectonic setting of the Early Miocene granitoids are still controversial although they are crucial to the study of the Alpine evolution of western Turkey.

The Early Miocene Alaçamdağ granites are one of the key plutons located in the boundary zone between the metamorphic basement (the Menderes Massif) and the structurally overlying ophiolitic rocks (the İzmir–Ankara Zone) (Fig. 1), and they have not been studied. In this paper, I provide petrographic, structural and geochronological data from the Alaçamdağ granites, aimed at elucidating their role in the origin and evolution of extensional detachment faults and continental extension in the Aegean region.

2. Overview: tectonic events in the Aegean region

The basement to the Neogene basins in the Aegean region is composed of various tectonic units amalgamated during Late Cretaceous to Eocene continental collision across the Neotethyan Ocean (Fig. 1). The most important basement rock unit in the region from the extensional tectonics point of view is represented by the metamorphic rocks exposed largely in the Menderes, Cyladic and Kazdağ massifs. The metamorphics share a common Mesozoic history and were involved in the same accretionary complex formation during Late Cretaceous to Early Tertiary times (Rimmelé *et al.* 2003*a*,*b*; Jolivet *et al.* 2004; Whitney *et al.* 2008); the presence of high pressure and low temperature rocks in the Menderes and Cycladic massifs has been attributed to this Alpine subduction event(s) (e.g. Oberhänsli *et al.* 1998; Candan *et al.* 2001; Okay, 2001; Rimmelé *et al.* 2003*b*; Ring & Layer, 2003; Jolivet *et al.* 2004; Whitney *et al.* 2008). Collisional events also caused the Eocene high temperature–medium pressure Barrovian-type main Menderes metamorphism during the southward translation of the Lycian nappes over the Menderes Massif area (e.g. Şengör, Satır & Akkök, 1984; Whitney & Bozkurt, 2002; Rimmelé *et al.* 2003*a*; Bozkurt, 2004; Erdoğan & Güngör, 2004). Nappe stacking has formed the crustal-scale compressional structures within the Menderes Massif, indicating a top-to-the-N–NNE movement during the main Menderes metamorphism (Hetzel *et al.* 1998; Bozkurt & Park,

https://doi.org/10.1017/S0016756809990719 Published online by Cambridge University Press

1999; Bozkurt & Satır, 2000; Whitney & Bozkurt, 2002) and cast doubt on the relationship between the main Menderes metamorphism and southward translation of the Lycian nappes.

The crust which had over-thickened during the collision collapsed due to southward roll-back of the Aegean trench and the region consequently underwent crustal extension (back-arc extension), during which the metamorphic rocks were exhumed and granitic magmatism occurred in the footwall of extensional shear zones and detachment faults (Jolivet, 2001; Le Pichon *et al.* 2002) (Fig. 1).

The Menderes Massif is one of the largest core complexes in the world and comprises three submassifs, separated by detachment faults and E–W-trending Plio-Quaternary graben systems, known as the northern, central and southern Menderes massifs (also termed Gördes, Ödemiş–Kiraz and Çine submassifs, respectively) (Fig. 1). The massif consists mainly of orthogneisses (traditionally known as augen gneisses), paragneisses, schists, quartzite and marbles, with differing metamorphic grade (Schuiling, 1962; Şengör, 1984; Bozkurt & Oberhänsli, 2001; Koralay *et al.* 2004). It is structurally overlain by the İzmir–Ankara Zone to the north and by the Lycian nappes to the south. There are reports of HP–LT rock assemblages (eclogites and blueschists) in the southern and central submassifs and they are interpreted as the eastern continuation of the Cycladic Massif (Oberhänsli *et al.* 1998; Ring, Laws & Bernet, 1999; Candan *et al.* 2001; Okay, 2001; Whitney *et al.* 2008). In the Aegean islands, the HP rocks occur in an approximately 500 km wide E–W-trending arcuate belt, exhumed by extrusion wedges and extensional detachment faults since Eocene times (Ring, Thomson & Bröcker, 2003; Ring *et al.* 2007; Ring & Kumerics, 2008). The present study is located in the northern Menderes Massif.

The Kazdağ Massif in northwestern Turkey consists of high-grade metamorphic rocks of gneiss, amphibolite and marble (Okay & Satır, 2000; Duru *et al.* 2004). Rb–Sr dating from the mylonitic shear zones and synextensional granitoids from the Kazdağ Massif revealed rapid exhumation along a north-dipping, top-to-the-north mylonitic shear zone that was active during Early (Okay & Satır, 2000) and Middle Miocene times (Cavazza, Okay & Zattin, 2009). The shear zone beneath the detachment fault is characterized by an approximately 2 km thick mylonite where ductile fabrics are progressively overprinted by brittle structures. The hanging-wall is composed of unmetamorphosed rocks of Çetmi mélange (Okay & Satır, 2000; Beccaletto *et al.* 2005; Cavazza, Okay & Zattin, 2009). The synextensional granitoids occur in a NE–SW-trending belt and are less deformed.

Radiometric dating of fault rocks and synextensional granites has constrained the timing of development of the Menderes and Cycladic metamorphic core complexes as Early to Late Miocene. The synextensional granites, which intrude different lithologies of the northern Menderes Massif, are Early Miocene in age. U–Pb SIMS and Ar–Ar data from the synextensional Koyunoba and Eğrigöz granites yield crystallization and cooling ages of around 20 Ma (Işık, Tekeli & Seyitoğlu, 2004; Ring & Collins, 2005) (Fig. 2). In the southern Aegean, the onset of the extensional detachments is Miocene (*c*. 24 to 8 Ma) on the islands of Crete, Tinos and Paros (Thomson, Stöckhert & Brix, 1999). In the central Menderes Massif, two small plutons, the Salihli and Turgutlu granodiorites, gave U–Pb crystallization ages of 16.1 ± 0.2 and 15.0 ± 0.3 Ma, respectively; they are interpreted as syn-tectonic granitoids emplaced in a top-to-the-NNE extensional shear zone (Hetzel *et al.* 1995*b*; Glodny & Hetzel, 2007). Similarly, in the Cycladic Massif, extension is manifested by the presence of Middle–Late Miocene (16–6 Ma) synextensional granitoids emplaced in the footwall of extensional detachment faults and along the NE-trending ductile shear zones (Pe-Piper, Kotopouli & Piper, 1997; Bröcker & Franz, 1998; Pe-Piper, 2000; Hejl, Riedl & Weingartner, 2002; Sanchez-Gomez, Avigad & Heimann, 2002; Ring *et al.* 2003; Ring & Layer, 2003). Although the Menderes and Cycladic massifs have many similarities, their geometry and timing of extensional individual detachments are in contrast to one another (Ring, Thomson & Bröcker, 2003). Detachments in the Cycladic Massif indicate a unique top-to-the-NNE shear sense and are consistent with an asymmetric extension (Gautier & Brun, 1994; Hetzel *et al.* 1995*b*). The Menderes Massif is, on the other hand, characterized by south- and north-dipping detachment faults. The evolution of these structures is controversial: (1) according to one school of thought, the massif is a typical asymmetric core complex exhumed in the footwall of a major fault, namely the Kale–Datça break-away fault (Seyitoğlu, Işık & Çemen, 2004), although no structural data were presented in favour of the model; (2) a second group argues for a symmetric extension (e.g. Hetzel *et al.* 1995*a*,*b*; Bozkurt, 2001; Gessner *et al.* 2001*a*,*b*; Lips *et al.* 2001; Ring *et al.* 2003; Çemen *et al.* 2005). Apatite fission track data from the Menderes Massif, which show regionally symmetric cooling patterns, are consistent with a bivergent extension model (Gessner *et al.* 2001*b*; Ring *et al.* 2003). These recent data indicate that the detachments in the Menderes Massif have different ages and evolutions, therefore their tectonic significance must be used with care. This highlights a need for the evaluation of existing models regarding the symmetry of Miocene continental extension in the massif area.

There have been several attempts to explain the origin and age of extension: (1) the orogenic or gravitational collapse model (Dewey, 1988; Seyitoğlu & Scott, 1996); this model assumes that the extension was a result of the collapse of over-thickened crust following the Latest Paleocene/Eocene collision. The model also explains extensive magmatic events as resulting from lithospheric delamination or asthenospheric upwelling (Aldanmaz *et al.* 2000; Dilek & Altunkaynak, 2007); (2) the tectonic escape model (Şengör, Görür &

https://doi.org/10.1017/S0016756809990719 Published online by Cambridge University Press

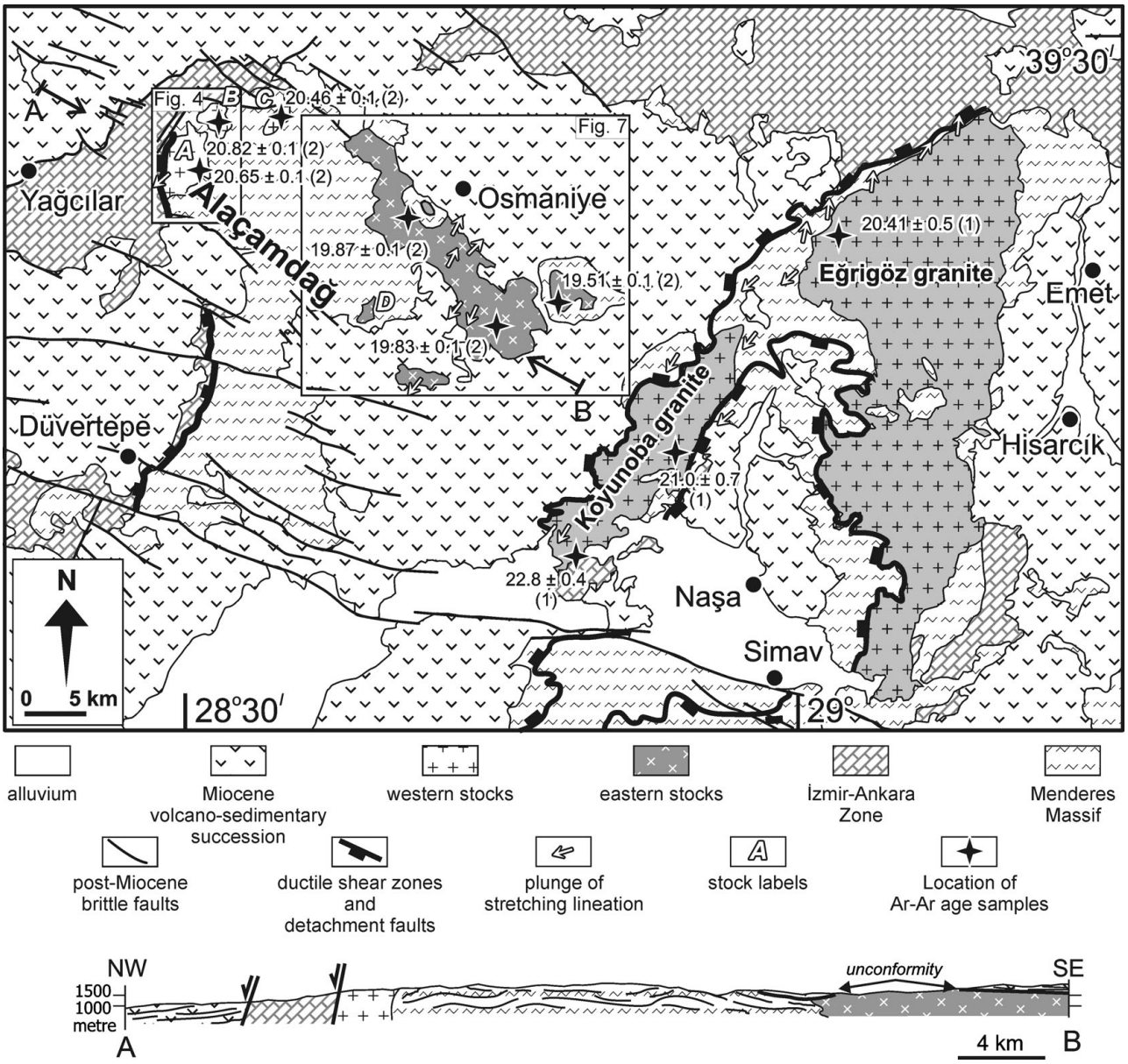

Figure 2. Geological map of the Alaçamdağ area and surroundings (modified from Akdeniz & Konak, 1979; Işık & Tekeli, 2001) and cross-section A–B (see map for location) showing contact relationships of the Alaçamdağ granites. Labels A, B, C and D on map refer to the stocks shown in Table 1. Ar–Ar age data sources: (1) Işık *et al.* 2004 and (2) this study. Locations of Figures 4 and 7 are also shown.

Şaroğlu, 1985); extension is explained by the westward escape of the Anatolian block along the boundary structures of the North Anatolian and East Anatolian Fault Zones that propagated since *c.* 13 to 11 Ma; (3) differential rates of convergence between the African Plate and the hanging-wall Anatolian Plate (Doglioni *et al.* 2002); in this model, the faster southeastward motion of Greece relative to Cyprus–Anatolia caused extension associated with a subduction zone, where the hanging-wall plate overrode the slab at different velocities; (4) roll-back of the Aegean subduction zone (Le Pichon & Angelier, 1979, 1981; Le Pichon, Bergerat & Roulet, 1988; Meulenkamp *et al.* 1988; Thomson, Stöckhert & Brix, 1998; Jolivet, 2001; Le Pichon *et al.* 2002; Tirel *et al.* 2004). The model assumes that subduction processes in the Aegean trench have been active throughout the Aegean region and roll-back of the subducting slab formed extensional back-arc basins (Le Pichon, Bergerat & Roulet, 1988; Buick, 1991). The model is also supported by the subduction signature and southward younging of magmatism in the Aegean region (Fytikas *et al.* 1979, 1984; Delaloye & Bingöl, 2000). However, timing of the onset of subduction and the position of the subducting slab during the extensional period are matters of debate (*c.* 13 Ma: Le Pichon & Angelier, 1979, 1981; *c.* 26 Ma: Meulenkamp *et al.* 1988; Early Tertiary: Spakman, Wortel & Vlaar, 1988; Eocene, flat subduction: Westaway, 2006; Late Oligocene, gently dipping oceanic slab: Kaya *et al.* 2007). Furthermore, recent research has revealed the possibility that the subduction events might have dated back to Mesozoic times (Van Hinsbergen *et al.* 2005; Jolivet & Brun, in press).

https://doi.org/10.1017/S0016756809990719 Published online by Cambridge University Press

3. Early Miocene granitoids in western Turkey

Early Miocene granitoids are exposed along a ~ 300 km wide discontinuous belt across the Sakarya Zone, İzmir–Ankara Zone and the northern Menderes Massif (Fig. 1). They display rhomb-shaped and circular outcrop patterns, with exposures ranging from a few kilometres to 480 km^2. The long axis of the rhomb-shaped granitoids commonly extends in a N–S and NE–SW direction (Kaya *et al.* 2007). Granitoids occur as shallow intrusions and are commonly characterized by narrow contact metamorphic aureoles within the host rocks. They are quartz monzonite, granodiorite, granite, quartz diorite and diorite in composition (e.g. Bingöl, Delaloye & Ataman, 1982; Altunkaynak & Yılmaz, 1998, 1999; Karacık & Yılmaz, 1998; Delaloye & Bingöl, 2000; Dilek & Altunkaynak, 2007; Aydoğan *et al.* 2008; Özgenç & İlbeyli, 2008; Boztuğ *et al.* 2009). Ductile deformation associated with the Early Miocene granitoids occurs spatially and temporally to a variable extent. Mylonitic zones locally envelop the undeformed and equigranular granite stocks, particularly where they are associated with, and intrusive into, the metamorphic rocks of the northern Menderes Massif. The Koyunoba and Eğrigöz plutons form the best examples of this type and intrude the orthogneisses of the Menderes Massif. Mylonites occur along the western and northern margins of the Koyunoba and Eğrigöz plutons, respectively. Mineral stretching lineations in both areas are consistent with a top-to-the-northeast sense of shear (Işık & Tekeli, 2001; Işık, Tekeli & Seyitoğlu, 2004; Ring & Collins, 2005; Thomson & Ring, 2006) (Fig. 2). The authors document overwhelming structural, geochronological and thermochronological evidence that the plutons are synextensional granitoids exhumed and cooled rapidly in the footwall of the Simav detachment fault during Early–Middle Miocene times. Similarly, limited data from the contact zones of other Early Miocene granitoids in the Sakarya Zone (e.g. the Kozak, Kestanbol and Eybek granitoids) suggest the presence of N–S- and NE–SW-trending semi-ductile to brittle shear zones and skarn mineralizations (Fig. 1) (Altunkaynak & Yılmaz, 1998, 1999; Akal & Helvacı, 1999; Hisarlı & Dolmaz, 2004; Yücel-Öztürk, Helvacı & Satır, 2005; Yılmaz, 2007). Apart from the extensional tectonic setting, there are also claims that the plutons were emplaced into the pull-apart areas along NE–SW-trending strike-slip shear zones associated with NNE–SSW- or NE–SW-directed extension (Kaya *et al.* 2007).

The Alaçamdağ granites form one of the Early Miocene granitoids in the region and occur to the west of Koyunoba and Eğrigöz granitoids. They are located along the boundary zone between the northern Menderes Massif and the İzmir–Ankara suture zone (Fig. 2). Unlike the general NE–SW trend of the Koyunoba and Eğrigöz plutons, the granites in the Alaçamdağ occur as two separate bodies and have NW–SE and N–S trends. More importantly, they have not been studied previously. I therefore present the results of new structural data from these granites and discuss their role and importance in the evolution of the Neogene crustal extension in the region.

4. The Alaçamdağ granites

The granites occur within the northern Menderes Massif, which consists of mica-quartz schist/phyllite, chlorite schist and minor marble intercalations. The metamorphic rocks are structurally overlain by the İzmir–Ankara Zone (Okay & Siyako, 1993). The zone is represented by Late Cretaceous to Paleocene mélange rocks with mountain-forming Mesozoic limestone olistoliths embedded in an extensively sheared matrix of sandstone and shale intercalations (Okay & Altıner, 2007). The mélange also locally includes radiolarite and spilite olistoliths and ultramafic/serpentinite slices. In the Alaçamdağ area, the İzmir–Ankara zone trends in an approximately E–W direction, although the zone has a NW–SE trend in the east and a NE–SW orientation in the west (Fig. 1). Rock units of the northern Menderes Massif and the İzmir–Ankara Zone are intruded by a number of granite stocks, named here the Alaçamdağ granites. The Miocene volcano-sedimentary succession overlies the older rocks unconformably and covers an area of hundreds of square kilometres surrounding the Alaçamdağ area (Fig. 2). It is made up of dacitic domes, lava flows, welded/non-welded ignimbrites and fluvio-lacustrine sedimentary rocks. The fluvio-lacustrine sediments occur as lenses at the lower parts of the succession and are replaced gradually upward by felsic volcanic rocks, mainly welded/non-welded ignimbrites. Geochronological data from similar rock units in the Bigadiç Basin indicate that the felsic volcanic rocks are Early Miocene (K–Ar biotite ages ranging from 20.2 to 19.0 Ma) (Erkül, Helvacı & Sözbilir, 2005*a*,*b*).

The Alaçamdağ granites form two major discontinuous outcrops (Fig. 2): the western and eastern stocks, which display distinct lithological and structural features. Although both stocks are mineralogically granite in composition, the western stock displays holocrystalline texture with minor porphyritic equivalents, whereas the eastern stock is characterized by a typical porphyritic texture. Exposed skarn zones are only associated with the western stock. The isolated outcrops of the western and eastern stocks display typical rhomb-shaped geometry with intrusion aspect ratios (l_m/w_m) ranging from 1.8 to 2.6 (Table 1). Ar–Ar biotite cooling ages of these intrusions range from 20.82 to 19.51 Ma (Fig. 2).

4.a. Ar–Ar dating of the Alaçamdağ granites

4.a.1. Analytical procedures

The Ar–Ar age determinations were performed in the geochronological laboratory of the Nevada Isotope

https://doi.org/10.1017/S0016756809990719 Published online by Cambridge University Press

Table 1. Kinematic aspects of isolated intrusions forming the Alaçamdağ granites

Stocks	Area covered (km^2)	Elongation	Rhomb shape	l_s (km)	w_s (km)	l_m (km)	w_m (km)	l_s/w_s	l_m/w_m
Western stocks									
A	11	N–S	Symmetric	4.5	3.2	6.2	2.8	1.4	2.2
B	3	N–S	Asymmetric			2.8	1.6		1.8
C	2	NE–SW	Symmetric	2.7	1.7	3.2	1.2	1.6	2.6
Eastern stocks									
D	1.5	NE–SW	Symmetric	2.5	1.8	2.9	1.1	1.4	2.6

l_s – length of pull-apart structure along strike, w_s – width perpendicular to strike, l_m – longest diagonal of the pull-apart structure; w_m, width perpendicular to l_m. Analogous experimental models are from Basile & Brun (1999). Refer to Figure 2 for location of stocks.

Table 2. $^{40}Ar/^{39}Ar$ analytical data for incremental heating experiments on biotites of the selected Alaçamdağ granite samples

Sample	Locality (UTM – Zone 35)	Stocks	Mineralogy	Texture of granites	Dated material	Total gas age* (Ma)	Plateau age (Ma)	Isochron age (Ma)
A-9	631542/4367877	Western	q, pf, plg, bio, zi, op	Equigranular	bio	21.28	20.98	20.82 ± 0.11
A-21	630390/4364466	Western	q, pf, plg, hnb, zi, op	Equigranular	bio	21.18	20.78	20.65 ± 0.11
A-40	636084/4368640	Western	q, pf, plg, bio, hnb, ti, op	Equigranular	bio	20.69	20.68	20.46 ± 0.12
A-11	644773/4360962	Eastern	q, pf, plg, hnb, zi, op	Porphyritic	bio	20.41	20.04	19.87 ± 0.08
A-50	651000/4353500	Eastern	q, pf, plg, bio, zi, ti, op	Protomylonitic	bio	20.22	20.02	19.83 ± 0.06
A-54	655413/4355019	Eastern	q, pf, plg, bio, zi, op	Porphyritic	bio	19.97	19.95	19.51 ± 0.11

q –quartz; pf – potassium feldspar; plg – plagioclase; hnb – hornblende; bio – biotite; ti – titanite; zi – zircon; op – opaque minerals
*Total gas age corresponds to K–Ar age.

Geochronology Laboratory, USA. Details of the analytical methods and data treatment are presented by Justet & Spell (2001) and Spell & McDougall (2003). Samples were run as conventional furnace step-heating analyses. This type of sample run produces what is referred to as an apparent age spectrum. 'Apparent' derives from the fact that ages on an age spectrum plot are calculated assuming that the non-radiogenic argon (often referred to as trapped, or initial argon) is atmospheric in isotopic composition ($^{40}Ar/^{36}Ar = 295.5$). If there is excess argon in the sample ($^{40}Ar/^{36}Ar > 295.5$) then these ages will be older than the actual age of the sample. U-shaped age spectra are commonly associated with excess argon (the first few and final few steps often have lower radiogenic yields, thus apparent ages calculated for these steps are affected more by any excess argon present), and this is often verified by isochron analysis, which utilizes the analytical data generated during the step heating run, but makes no assumption regarding the composition of the non-radiogenic argon. Thus, isochrons can verify (or rule out) excess argon, and isochron ages are usually preferred if a statistically valid regression is obtained (as indicated by an acceptably low MSWD value). If such a sample yields no reliable isochron, the best estimate of the age is that the minimum on the age spectrum is a maximum age for the sample (it could be affected by excess argon, the extent depending on the radiogenic yield). $^{40}Ar/^{39}Ar$ total gas ages are equivalent to K–Ar ages. Plateau ages are sometimes found; these are simply a segment of the age spectrum which consists of three or more steps, comprising > 50 % of the total gas released, which overlap in age at the $\pm 2\sigma$ analytical error level (not including the J-factor error, which is common to all steps). Such ages are preferred to total gas or maximum ages if obtained. However, in general, an isochron age is the best estimate of the age of a sample, even if a plateau age is obtained.

4.a.2. ^{40}Ar–^{39}Ar geochronology

Ar–Ar geochronology was applied on the biotite samples of the Alaçamdağ granites (Table 2). The results of the $^{40}Ar/^{39}Ar$ incremental heating experiments on granite sample A-9 are nearly ideally flat and concordant, with the exception of some higher ages in the initial ~ 10 % of gas released, and the final ~ 1 % of gas released. If these steps are included, the sample does have an overall U-shaped age spectrum, despite the presence of a plateau segment. The total gas age for this sample is 21.3 ± 0.1 Ma. Steps 3–10 (88 % of the total ^{39}Ar released) define a plateau with an age of 21.0 ± 0.1 Ma. Steps 2–10 (96 % of the total ^{39}Ar released) yield an isochron age of 20.8 ± 0.1 Ma. The isochron indicates the presence of excess argon (initial $^{40}Ar/^{36}Ar = 312.3 \pm 1.3$) in this sample, thus the isochron age is youngest (age spectrum ages are calculated assuming $^{40}Ar/^{36}Ar = 295.5$). The isochron age was considered the most accurate and reliable for this sample (Fig. 3).

The $^{40}Ar/^{39}Ar$ incremental heating experiment results for sample A-21 are nearly flat and concordant, with the exception of some higher ages. The total gas age for this sample is 21.3 ± 0.1 Ma. Steps 8–10 (50 % of the total ^{39}Ar released) define a plateau with an age of 20.8 ± 0.1 Ma. Steps 8–12 (54 % of the total ^{39}Ar released) yield an isochron age of 20.7 ± 0.1 Ma. The isochron age of 20.7 ± 0.1 Ma is considered the most reliable for sample A-21 (Fig. 3).

The data for sample A-40 have a more discordant age spectrum than those for sample A-21. The total gas age is 20.7 ± 0.1 Ma. Steps 6–10 (58 % of the total ^{39}Ar

https://doi.org/10.1017/S0016756809990719 Published online by Cambridge University Press

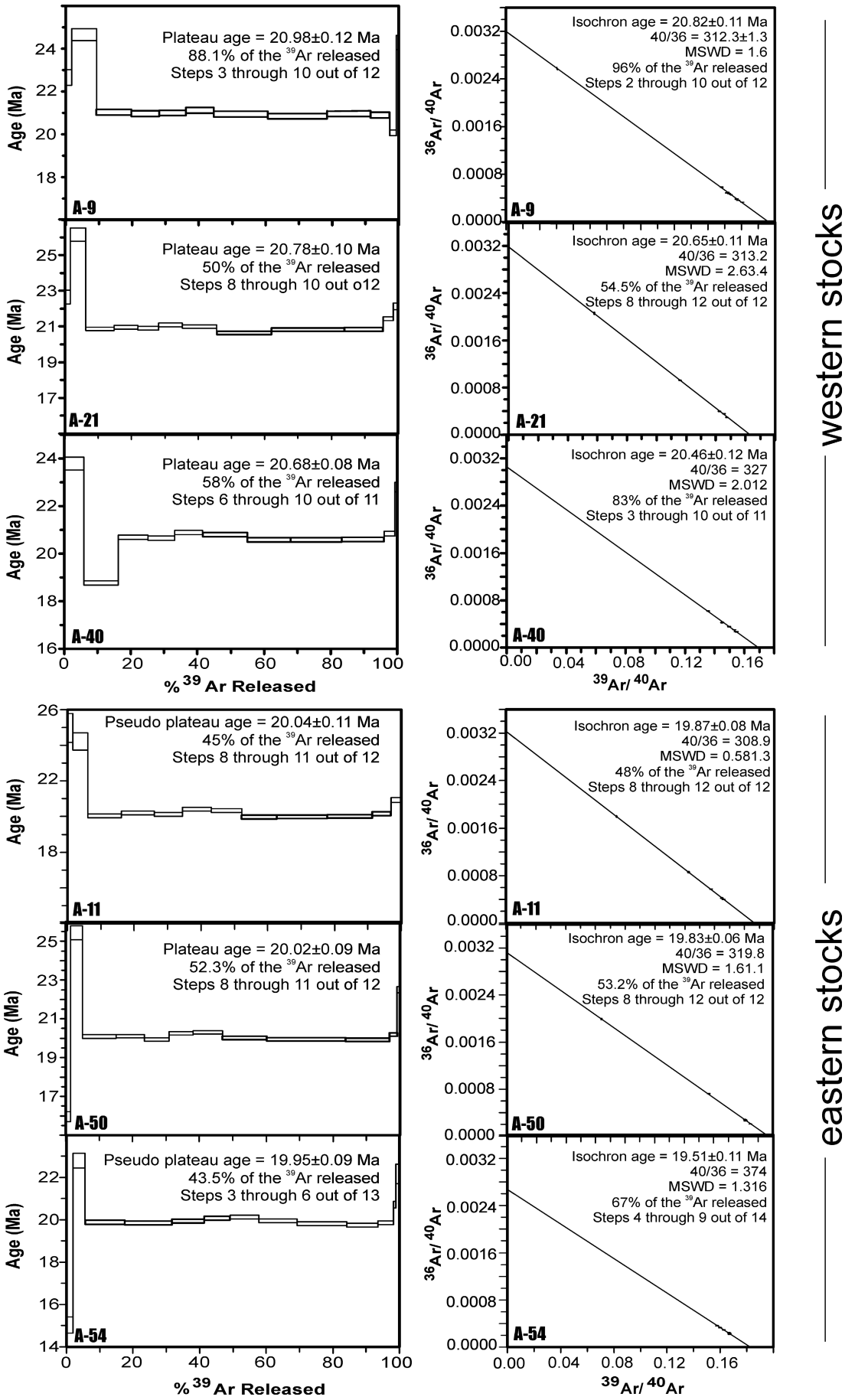

Figure 3. Ar–Ar age spectra and isochron diagrams of the dated samples of the Alaçamdağ granites.

https://doi.org/10.1017/S0016756809990719 Published online by Cambridge University Press

released) define a plateau with an age of 20.7 ± 0.1 Ma. Steps 3–10 (83 % of the total ^{39}Ar released) yield an isochron age of 20.5 ± 0.1 Ma. The isochron age of 20.5 ± 0.1 Ma is considered the most reliable (Fig. 3).

The age spectrum of sample A-11 is slightly discordant. The total gas age is 20.4 ± 0.1 Ma. The plateau defined comprises a smaller percentage of the total gas released (45 %) and is thus referred to as a 'pseudo-plateau', since this is less than the desired 50 % minimum. The pseudo-plateau age (20.0 ± 0.1 Ma) is slightly younger than the total gas age. An isochron is defined by steps 8–12 (48 % of the total ^{39}Ar released) and yields an age of 19.9 ± 0.1 Ma and initial ^{40}Ar/^{36}Ar = 308.9 ± 1.3, thus suggesting the presence of excess argon. Therefore, the isochron age is considered the most accurate and reliable for this sample, although > 50 % of the gas released defines an isochron. In this case the ages are consistent with what would be expected for excess argon (isochron age younger than total gas or plateau ages) and the isochron is defined by a significant number of data points (n = 5), which have a good spread (Fig. 3).

The data for sample A-50 are nearly ideally flat and concordant. The total gas age of this sample is 20.2 ± 0.1 Ma. Steps 8–11 (52 % of the total ^{39}Ar released) define a plateau with an age of 20.0 ± 0.1 Ma. Steps 8–12 (53 % of the total ^{39}Ar released) yield an isochron age of 19.8 ± 0.1 Ma. The isochron age is considered the most reliable (Fig. 3).

The data for the sample A-54 are again similar to those described above for the A-50 biotite ages. The total gas age of this sample is 20.0 ± 0.1 Ma. Steps 3–6 (43 % of the total ^{39}Ar released) define a plateau with an age of 20.0 ± 0.1 Ma. Steps 4–9 (67 % of the total ^{39}Ar released) yield an isochron age of 19.5 ± 0.1 Ma, which is the most reliable for this sample (Fig. 3).

4.b. Western stocks

The western stocks comprise a number of N–S- and NNE–SSW-trending outcrops and cover a total area of about 16 km^2 to the north of the Alaçamdağ (Fig. 2). They have elliptical or oval-shaped map views and consist of equigranular and porphyritic granites, and aplitic dykes. The granites intrude schists of the Menderes Massif and the clastic sediments and recrystallized limestones of the İzmir–Ankara Zone. The largest of these stocks trends approximately N–S, has a rhomb-shape and is exposed along a fault contact that juxtaposes the İzmir–Ankara Zone in the hanging-wall to the west with the rocks of the Menderes Massif in footwall to the east (Fig. 4). The contact with the recrystallized limestones along the western margin is characterized by local skarn occurrences, defined by garnet, pyroxene, epidote and pyrite mineralizations, and iron oxide disseminations (Fig. 5a). Along the eastern margin, the stock is intrusive into the mica schists and quartzites that are locally transformed into hornfelsic rocks. Aplitic dykes are commonly along the marginal zones and the structurally upper parts of the stock. The dykes commonly occur and cut both equigranular granites and the host-rock quartz-schists within a 100 m wide contact zone. Porphyritic granites occur as up to 1 m wide NE–SW-trending dykes, more or less parallel to the contact zone between the western stock and recrystallized limestones. They are particularly common and intrude the clastic sediments and the recrystallized limestones of the İzmir–Ankara Zone.

Granites display holocrystalline texture and commonly contain circular, elongate and oval-shaped mafic microgranular enclaves with sizes ranging from a few centimetres to 2 m, without any evidence of internal strain. The modal mineralogical composition of holocrystalline granite samples displays a restricted range of granitic to minor granodioritic compositions (Streckeisen, 1976) (Fig. 6a). Quartz (30–40 %) is typically anhedral and interstitial. Orthoclase (30–60 %) displays Carlsbad twinning and occurs as tabular prismatic crystals. Plagioclase (40–70 %) is commonly subhedral and is altered to sericite. Feldspars may locally have biotite and hornblende inclusions. Biotite, the main mafic phase, forms about 10–30 % of bulk-rock samples and contains small inclusions of zircon and apatite. Hornblende (5–10 %) consists of subhedral to anhedral crystals, displaying characteristic cleavage and greenish pleochroism. Apatite, sphene, zircon and opaque minerals form accessory phases within the granite samples. Where porphyritic texture is evident, the granites contain potassium feldspar megacrysts up to 0.5 cm long within a fine- to medium-grained groundmass of rock-forming minerals. Aplitic dykes are distinguished by their microcrystalline texture and are made up of quartz, plagioclase and potassium feldspar, minor mafic minerals of biotite and hornblende, and accessory phases. Alteration of feldspars to sericite and kaolinite is characteristic. Equigranular granites of the western stocks have yielded Ar–Ar cooling ages of 20.82 ± 0.1, 20.65 ± 0.1 and 20.46 ± 0.1 Ma from biotite extract (Fig. 2).

4.c. Eastern stocks

The eastern stocks are characterized by porphyritic granites and aplitic dykes of various sizes and cover a total area of about 65 km^2. They comprise several bodies of variable size and define a belt trending approximately NW–SE (Fig. 7). The largest of these is a 19 km long and 5 km wide elongate body of porphyritic granite, which intrudes the quartz-mica schists of the metamorphic basement. The contact zone is sharp, displays intrusive relationships at the centimetre scale and lacks skarn mineralizations. Aplitic dykes (up to 50 cm wide) in this contact zone (about 50 m wide) cut the porphyritic granites and the foliation of schists (Fig. 5b). The granite displays a typical undeformed porphyritic texture in the northwest, but becomes deformed and mylonitized gradually southeastward and structurally upwards towards the contact with the rocks of the İzmir–Ankara Zone (Fig. 7). The

https://doi.org/10.1017/S0016756809990719 Published online by Cambridge University Press

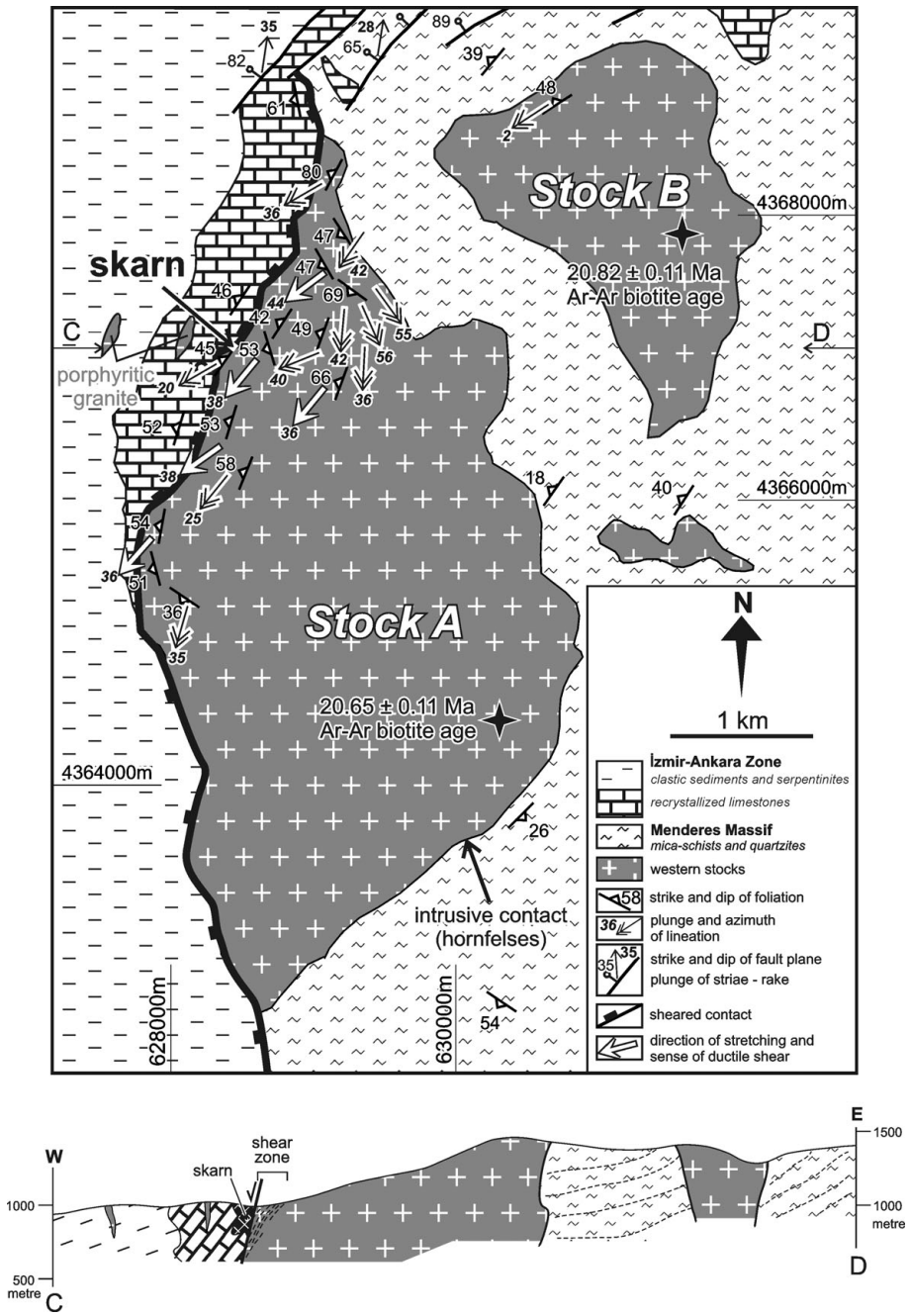

Figure 4. Geological map and cross-section C–D (see map for location) showing the western stocks in the Alaçamdağ area. See Figure 2 for location of the map. Map coordinates: Universal Transverse Mercator (UTM) projection, zone 35.

contact relationship with the İzmir–Ankara zone is unfortunately not observed, owing to the younger volcano-sedimentary cover. Along the structurally upper northeastern margin, the mylonitized granites are unconformably overlain by the undeformed and flat-lying ignimbrites. There is also a NE–SW-trending small stock to the southeast of the Alaçamdağ area, covering an area of about 1.5 km^2 (Fig. 7). It is made up of undeformed porphyritic granites and intrudes the quartz-mica schists of the metamorphic basement.

The mineralogical compositions of the eastern and western stocks are very similar. A major distinction in the east is the presence of abundant potassium feldspar megacrysts up to 5 cm long. Porphyritic granites consist of plagioclase, potassium feldspar, quartz, biotite, hornblende, and minor apatite, zircon and opaque minerals (Fig. 8a). Argillic/sericitic alteration in feldspars is common. Aplitic dykes are characterized by the microcrystalline texture formed by felsic minerals and minor mafic minerals.

Ar–Ar dating from the undeformed samples of the eastern stocks yielded cooling ages of 19.87 ± 0.1 and 19.51 ± 0.1 Ma from a biotite extract (Fig. 2). A mylonitized granite sample from the eastern stocks gave an Ar–Ar biotite age of 19.83 ± 0.1 Ma, which can be correlated with the cooling ages of the undeformed granite samples.

https://doi.org/10.1017/S0016756809990719 Published online by Cambridge University Press

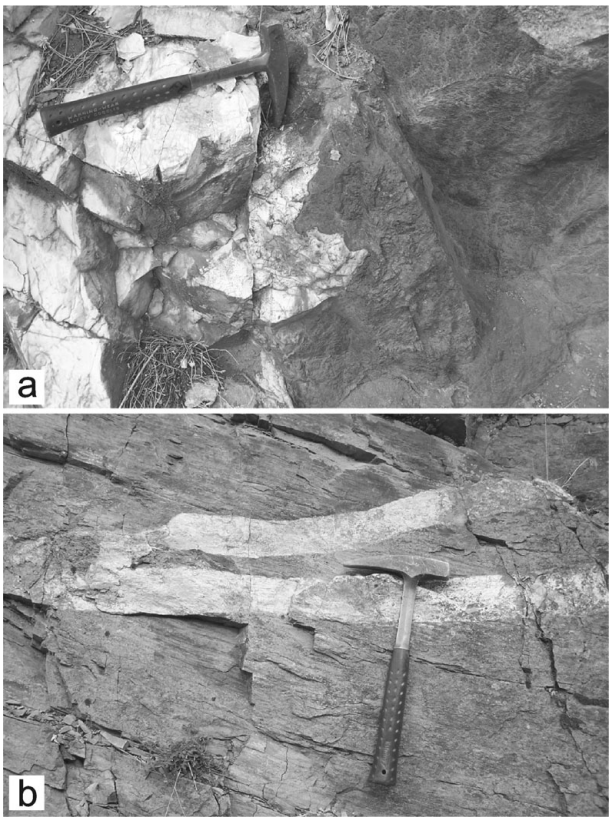

Figure 5. Intrusive contact zones of the western and eastern stocks. (a) Skarn zone comprising iron oxide disseminations along the contact between recrystallized limestones and western stocks (UTM coordinate 35S-628200/4367000). (b) Mica schists intruded by aplitic dykes associated with the eastern stocks (UTM coordinate 35S-645370/4361650). Hammer is 32 cm long. A colour version of this figure is available in online Supplementary Material at http://www.cambridge.org/journals/geo.

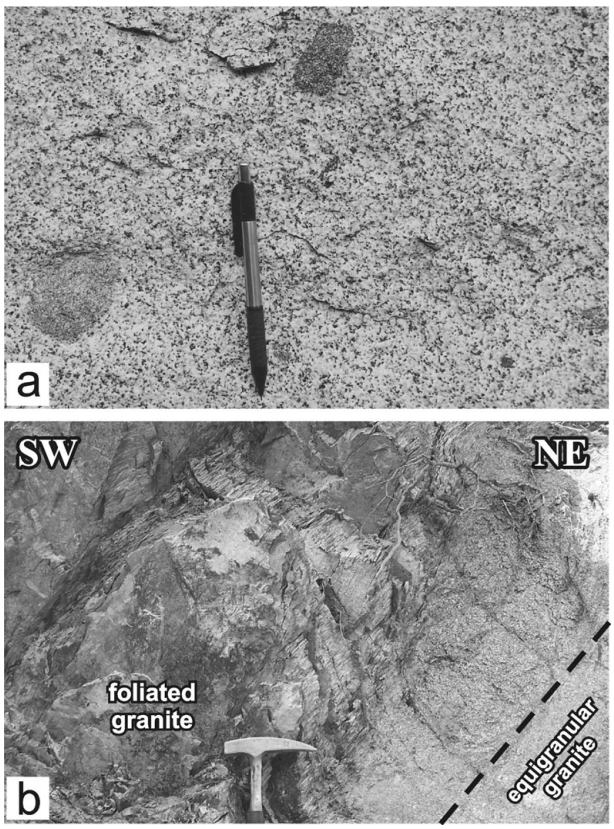

Figure 6. Mesoscopic appearance of the western stocks. (a) Equigranular granites including variably shaped mafic microgranular enclaves. Pen is 13 cm long (UTM coordinate 35S-630050/4365375). (b) Contact relationship between equigranular and foliated granites of the western stocks. Dashed line indicates the contact. Head of hammer is 16 cm long (UTM coordinate 35S-628000/4365470). A colour version of this figure is available in online Supplementary Material at http://www.cambridge.org/journals/geo.

5. Deformation in the Alaçamdağ granites

The two bodies of the granitic rocks in the Alaçamdağ area are deformed in two shear zones with differing geometries, deformation patterns, structural elements and kinematics: (1) the western shear zone and (2) eastern shear zone. The characteristics of each zone will be given in the following sections.

5.a. Western shear zone

The western shear zone trends in a NE–SW direction and occurs in the footwall of fault contact between the western granite and recrystallized limestones (Fig. 4). In the contact zone, the granites are transformed gradually into mylonites (Fig. 6b). The shear zone is relatively narrow and has a maximum width of about 800 m. It is mainly defined by more or less uniform and planar mylonitic foliation, and mineral stretching lineation. The domain spacing (microlithons) between individual foliation planes (cleavage seams) in the lower structural levels may reach up to 1 m, but the foliation gradually becomes penetrative westwards towards structurally upper horizons with a pronounced decrease in the thickness of individual microlithons (in the order of millimetres). Both the mylonitic foliation and lineation are defined by the preferred parallel alignment of strongly elongated and flattened quartz and feldspar grains, and sericite and biotite flakes. Strike of the foliation is commonly parallel to orientation of the fault contact (N45°E) but there are local areas with NW–SE-striking (N45°W) foliation planes, almost perpendicular to the general trend. They dip steeply (35° to 85°) towards the northwest or southwest. The mineral lineation trends in a NE–SW direction and plunges southwestward at gentle to moderate angles (2–56°; Fig. 9a). Abundance of chlorite increases toward the western margin of the shear zone, suggesting the role and importance of retrogressive processes in the shear zone.

The progressive deformation of the mylonitic rocks and consequent brittle overprint resulted in the formation of ultramylonites at the immediate footwall of the fault contact. Two types of ultramylonites, based on their mineralogy, are defined as quartz-rich and sericite-rich ultramylonites. Quartz-rich ultramylonites occur commonly at the structurally lower parts towards the undeformed section of the granites and grade into

https://doi.org/10.1017/S0016756809990719 Published online by Cambridge University Press

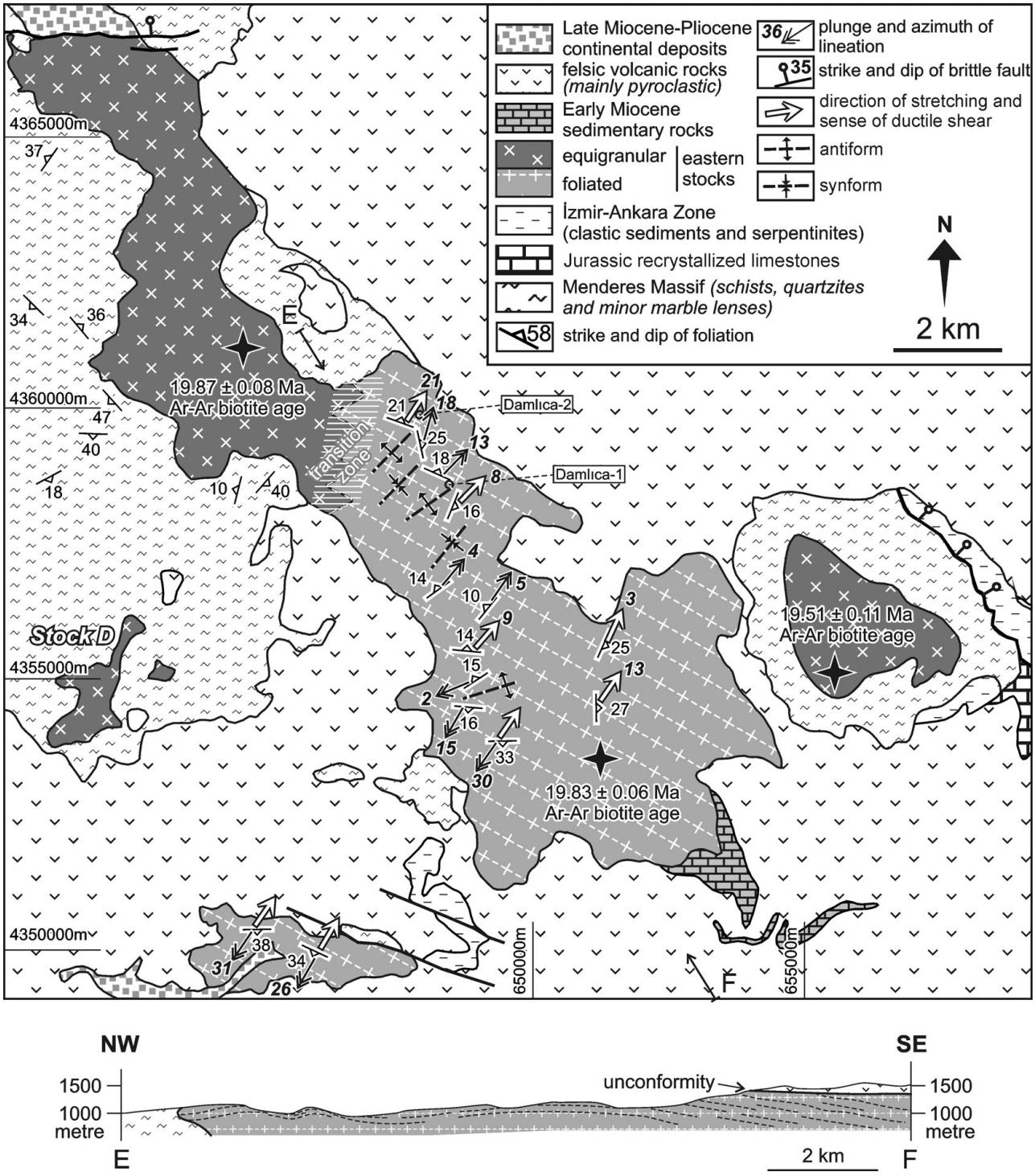

Figure 7. Geological map and cross-section showing the eastern stocks in the Alaçamdağ area. See Figure 2 for location of the map. Damlıca-1 and Damlıca-2 are stations of brittle fault measurements. Map coordinates: Universal Transverse Mercator (UTM) projection, zone 35.

sericite-rich ultramylonites towards the marginal parts of the shear zone.

The ultramylonites are recognized by intense deformation and strong alignment of abundant biotite and dynamically recrystallized quartz grains, and minor hornblende grains. Quartz forms about 60–70 % of matrix grains and commonly occurs as ribbons almost parallel to main foliation in the rock. The ultramylonites display S–C fabrics where C-foliation is characterized by the alternation of quartz- and biotite-rich domains, whereas S-foliation is characterized by elongate quartz sub-grains that define a perfect grain-shape foliation oblique to C-surfaces (Fig. 8b). Dynamically recrystallized quartz grains have serrated and sutured boundaries, indicating grain boundary migration processes (Tullis & Yund, 1982). Microfaults, fractures and veins also cut the foliation at a high angle (~ 60° towards the southwest);

https://doi.org/10.1017/S0016756809990719 Published online by Cambridge University Press

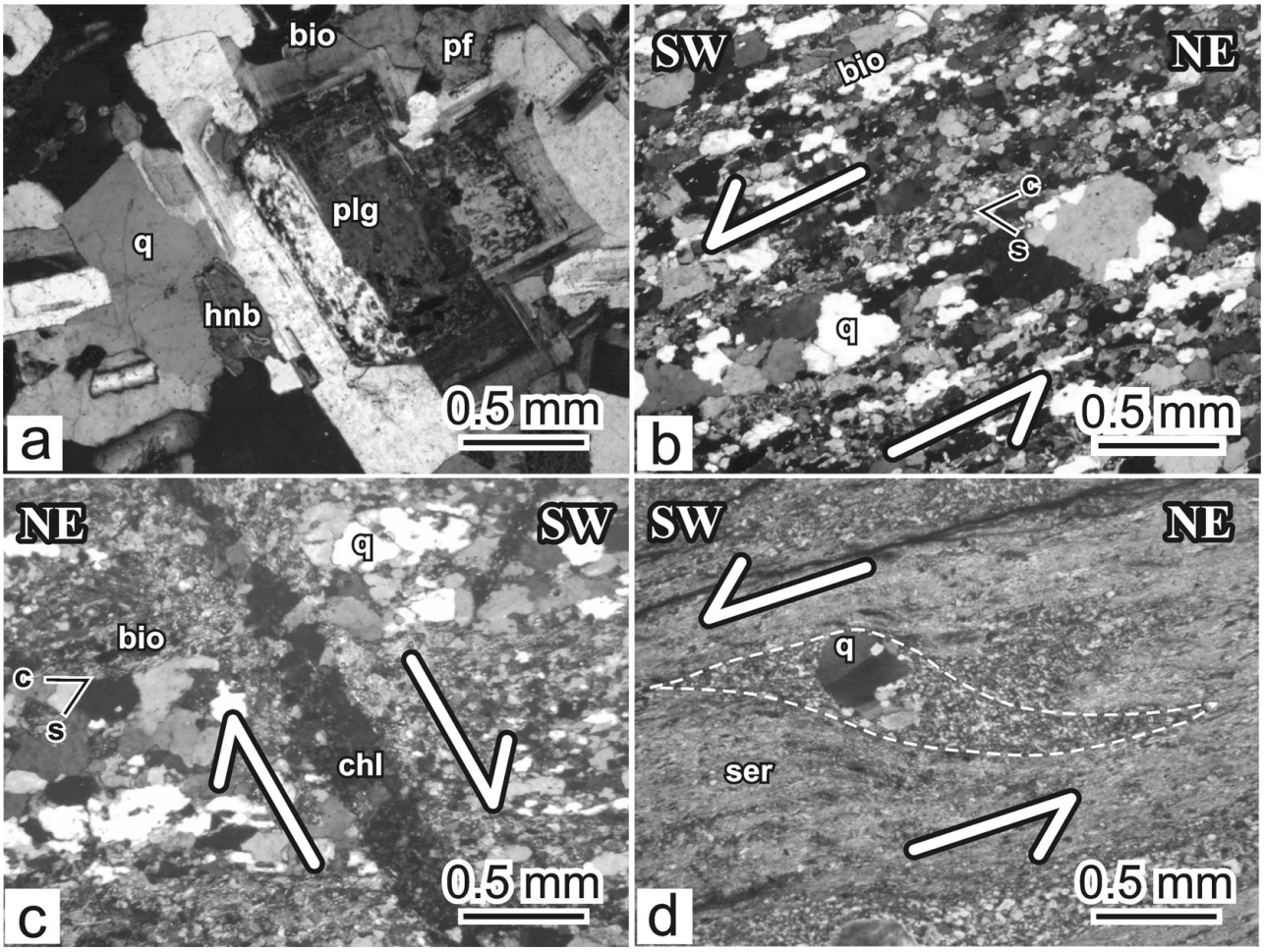

Figure 8. Photomicrographs of magmatic textures and deformational structures within the western stocks. (a) Holocrystalline granites without any evidence of magmatic and deformational foliation. (b) Photomicrograph of quartz-rich mylonite. Mylonitic foliation C is defined by quartz ribbon and trails of biotite, while obliquely oriented fabric S is formed by elongated recrystallized quartz grains. The angle between S and C surfaces is consistent with sinistral shearing. (c) Microfault overprinting the mylonitic foliation defined by trails of biotite and quartz grains, indicating a normal displacement. Microfault is filled by chlorite after biotite. Biotite grains are locally dragged and smeared along microfaults. (d) Mantled quartz porphyroclasts recrystallized into the smaller grains. Note that sericite forms major proportion of matrix. Microfaults, oblique quartz-grain-shape foliation and asymmetric mantled porphyroclasts indicate a top-to-the-SW sense of shear. bio – biotite; q – quartz; plg – plagioclase; pf – potassium feldspar; hnb – hornblende; chl – chlorite; ser – sericite. A colour version of this figure is available in online Supplementary Material at http://www.cambridge.org/journals/geo.

their offset is in the order of < 0.5 cm (Fig. 8c). The fractures are commonly filled by biotite, retrograde chlorite and minor quartz and feldspars. Biotites and chlorites locally exhibit drag folds, indicating a normal shear sense of motion with respect to the present-day geometry of the fractures.

Sericite-rich ultramylonites consist of abundant sericite (over 90 %) and minor quartz grains of differing sizes. This is recognized by high birefringence colours and flattened/undulated flakes, which mainly define the mylonitic foliation planes. Quartz grains occur as mantled porphyroclasts recrystallized into the smaller grains and include fractures oblique to foliation, indicating incipient mylonitization of the quartz porphyroclasts (Bestmann, Prior & Veltkamp, 2004) (Fig. 8d). Mantled quartz porphyroclasts commonly display undulose extinction and form asymmetric trails of small quartz grains derived from the porphyroclast. They exhibit typical sigma-type geometry (cf. Passchier & Trouw, 2005). Shear sense indicators, including quartz grain-shape foliation, asymmetric mantled quartz porphyroclasts and microfaults with normal offsets, are all consistent in indicating a top-to-the-southwest sense of shear.

5.b. Eastern shear zone

The eastern shear zone is represented by the mylonitized granitic and aplitic rocks exposed on the structurally upper part of the NW–SE-trending stocks (Fig. 7). Equigranular granites pass gradually into the strongly foliated granites towards the southeast within a zone a few hundred metres wide. The domain spacing (microlithons) between individual foliation planes (cleavage seams) is variable and ranges from a few tens of centimetres to a metre. The attitudes of the foliation planes define a series of alternating meso- to map-scale antiforms and synforms with approximately NE–SW-trending and gently NE-plunging axes, therefore the strike of the foliation varies between N–S and NE–SW,

https://doi.org/10.1017/S0016756809990719 Published online by Cambridge University Press

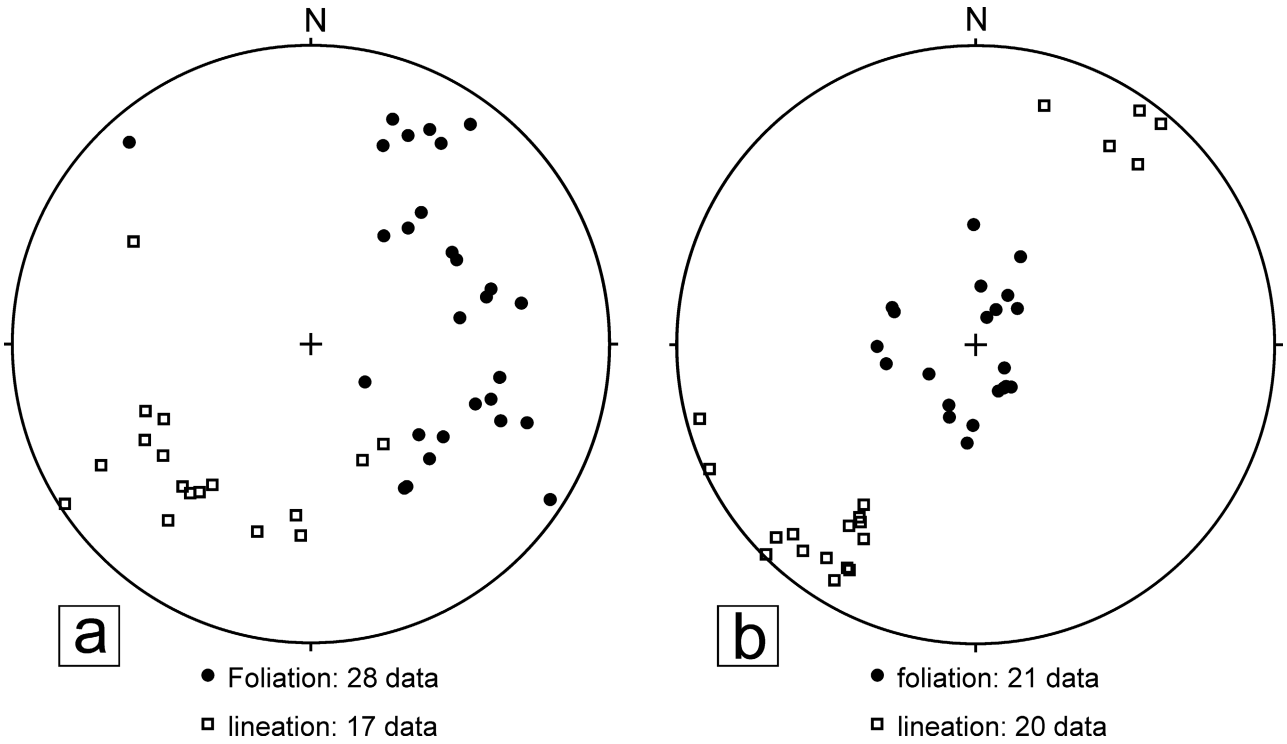

Figure 9. Lower hemisphere equal-area stereographic plots of poles to mylonitic foliation and lineation in the (a) western and (b) eastern shear zones.

with gentle to moderate (8–33°) dips towards either the northwest or southeast (Figs 7, 9b, 10a). The most striking feature is the parallelism between the fold axes and the local stretching lineation. The mineral stretching lineation is well expressed in the plane of quartz-rich foliation planes and is defined by the preferred parallel alignment of strongly elongated and flattened quartz and minor biotite and/or chlorite grains (Fig. 10b). The lineation plunges at gentle to moderate angles (1–20°) in the northern part of the foliated granites, while it is steeper in the southern part (27 to 31°) (Fig. 9b). C'-type shear band foliation also occurs sporadically and is oriented oblique to the foliation plane at an angle of ~ 40–43° (Fig. 10c). It commonly occurs as discontinuous surfaces and terminates in the quartz-rich domains. The angular relationship between C'-type shear band foliation and penetrative C-type foliation indicates a top-to-the-northeast shear sense. The eastern shear zone also contains deformed aplitic dykes that predominantly occur on the structurally upper or marginal zones of the granites. The dykes are a few tens of centimetres thick and cut pre-existing foliation planes within the porphyritic granites (Fig. 10d). The cross-cutting dykes are also foliated and occur as tapered, lens-shaped intrusions having long axes subparallel to pervasive foliation. Foliation in the aplitic dykes is defined by parallel alignment of quartz-rich domains and aligned mafic minerals.

In the northwestern exposures of the largest NW-trending stock, porphyritic granites are holocrystalline, but in the transition zone they contain plagioclase and potassium feldspars surrounded by recrystallized polygonal quartz grains (Figs 7, 11a). In the southeastern exposures, foliated granites are typical protomylonites with about 10–30 % matrix. Mylonitic zones with relatively fine-grained and foliated fabrics occur locally within the protomylonites. The feldspars occur in a core-and-mantle structure with core feldspar porphyroclasts (plagioclase and orthoclase) surrounded by a mantle of recrystallized quartz grains and kinked biotite flakes (Fig. 11b). Feldspars are fractured, display undulose extinction and form angular grains, suggesting relatively brittle deformation, while the matrix grains behaved in a rather ductile manner. In some thin-sections, the porphyroclast boundaries are offset by grain-scale faults; the fault zones at microscopic scale are defined by dynamic recrystallization of quartz and biotite, and retrogressive chlorite. Transformation of biotites into chlorite is a common phenomenon. Feldspar porphyroclasts usually form rounded, rolled, symmetric and asymmetric grains, where asymmetry defines typical sigma-type porphyroclasts with recrystallized tails where core potassium feldspars are mantled by recrystallized quartz and feldspar grains (Fig. 11c). Shear bands in the protomylonites are mainly recognized by fine-grained and elongate lenses of recrystallized quartz and trails of biotites (Fig. 11d). Biotites are dynamically recrystallized into smaller grains and are smeared out along shear planes oblique to the main foliation. Larger feldspar porphyroclasts show evidence of brittle deformation with grain-scale faults, defining a book-shelf structure or domino-type asymmetric boudins (cf. Goscombe & Passchier, 2003; Passchier & Coelho, 2006). The angle between the boudin plane and the boudin surface (Θ) is about 65° (Fig. 11e). Biotites in the mylonites define typical mica

https://doi.org/10.1017/S0016756809990719 Published online by Cambridge University Press

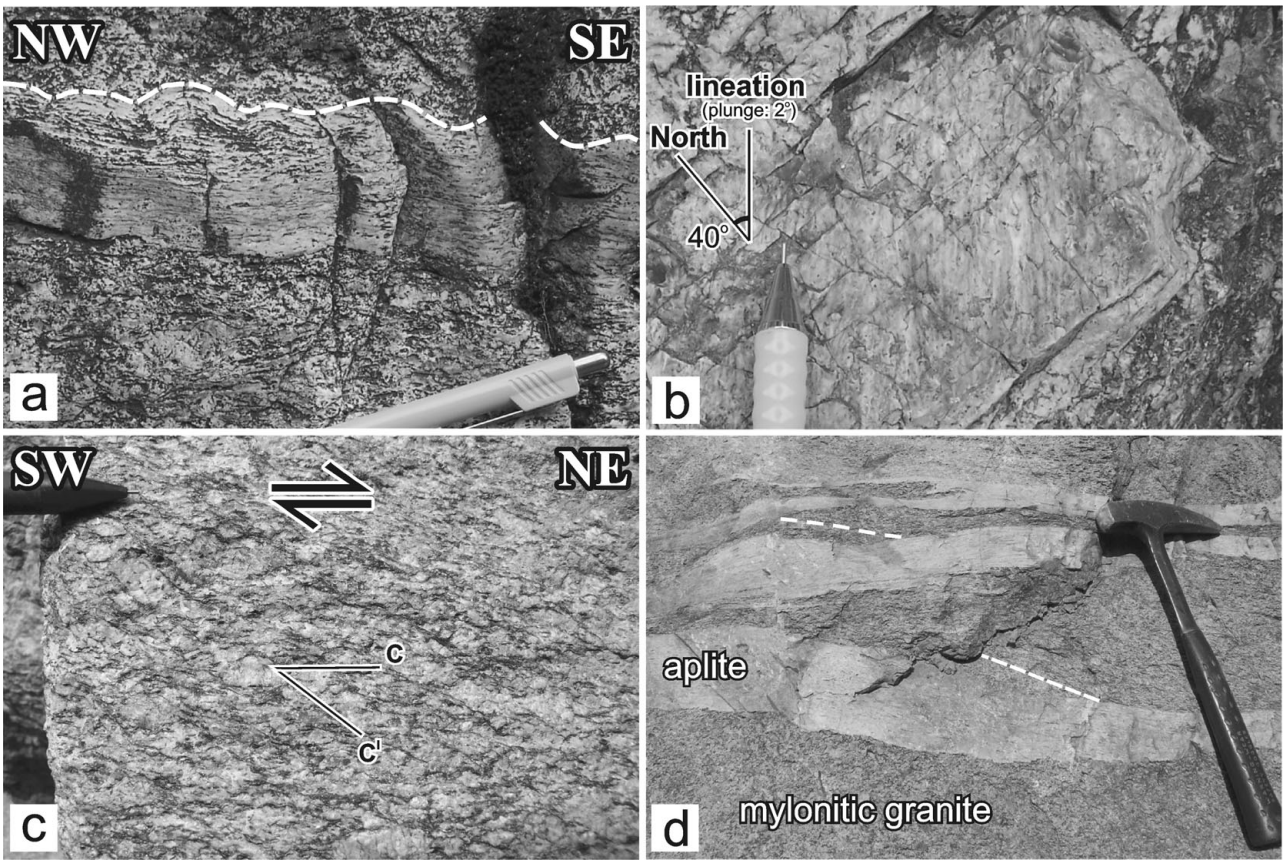

Figure 10. Field photographs of deformed granites in the eastern shear zone. (a) Mesoscopic-scale symmetrical folds (dashed line) enclosed by non-folded and near-planar foliations. Outcrop view is about parallel to foliation and normal to lineation. Pen is 1 cm thick (UTM coordinate 35S-648425/4355750). (b) Stretching lineations defined by elongate quartz grains and chlorite after biotite (UTM coordinate 35S-648025/4357400). (c) C'-type shear bands with normal sense of movement, indicating a top-to-the-northeast shear sense (UTM coordinate 35S-648025/4357400). (d) Tapered and lens-shaped mylonitic aplite dykes cutting the pre-existing foliation planes (white dashed line) of the mylonitic granites. Note that the intruding aplitic dykes are progressively deformed together with the mylonitic granites (UTM coordinate 35S-648560/4358760). A colour version of this figure is available in online Supplementary Material at http://www.cambridge.org/journals/geo.

fish structures (Fig. 11f) and occur as lozenge-shaped grains in a stair-step geometry defined by recrystallized tails. The kinematic indicators described above all indicate a top-to-the-northeast sense of shearing.

Brittle structures, mostly mesoscopic-scale faults, are common features of mylonitic granites. They occur as a series of oblique to normal faults, striking in NNE–SSW, NE–SW and NW–SE directions. They dip steeply with angles ranging between 46 and 87°. Where observed, slickenlines on the fault planes are predominantly parallel or slightly oblique to the general orientation of the mineral stretching lineations, thus attesting to a genetic link between the two sets of structures. Analyses of the two different sets of fault data were carried out separately, using the direct inversion method (INVDIR) of Angelier (1984, 1990) (Table 3). The method consists of determining the best-fitting reduced palaeostress tensor for a given fault dataset. All inversion results include the orientation (trend and plunge) of the principal stress axes and the stress ratio $[R = (\sigma_2 - \sigma_1)/(\sigma_3 - \sigma_1)]$, a linear quantity describing relative stress magnitudes. The stress axes σ_1, σ_2 and σ_3 correspond to maximum, intermediate and minimum principal stress axes, respectively. These parameters were computed using the TENSOR computer program developed by Angelier (1989).

For the station Damlıca-1, the calculated σ_1 trends 010° and plunges at 69°, while the σ_2 and σ_3 axes have average attitudes of 274°/02° and 183°/21°, respectively (Fig. 12; Table 3). The calculated principal stress axes from the normal faults in the station Damlıca-2 have the following attitudes: $\sigma_1 = 088°/71°$, $\sigma_2 = 233°/16°$, and $\sigma_3 = 326°/10°$. The computed results for the fault-slip data indicate a NW–SE and N–S extension (Fig. 12). Computed stress ratios for the fault-slip data of the Damlıca-1 and Damlıca-2 stations are 0.368 and 0.578, respectively. Based on these stress ratios and principal stress axes, stress tensors can be classified into pure extension (cf. Delvaux *et al.* 1995; Tranos *et al.* 2008). These results suggest that the oblique and normal faults overprinting the mylonitic fabrics have developed under NW–SE- and N–S-directed extension.

6. Discussion

6.a. Emplacement mode of the Alaçamdağ granites

The presence of coeval extrusive and hypabyssal rocks, narrow contact metamorphic aureoles and/or skarn

https://doi.org/10.1017/S0016756809990719 Published online by Cambridge University Press

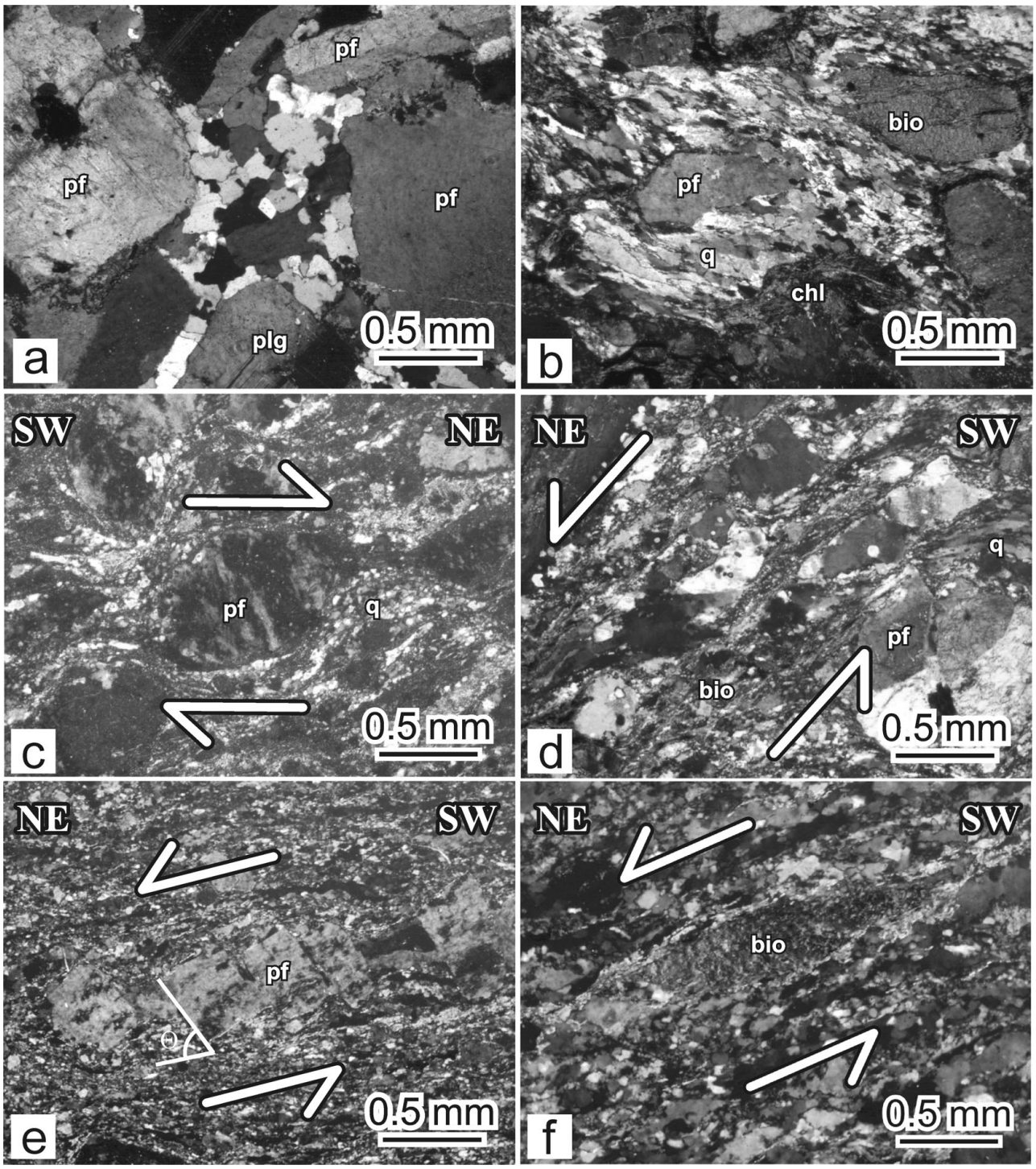

Figure 11. Photomicrographs of magmatic textures and deformational structures within the eastern stocks. (a) Crystals of plagioclase and potassium feldspars enclosing recrystallized polygonal grains of quartz near the transitional zone. (b) Dynamically recrystallized elongate quartz grains and smeared biotite trails surrounding brittlely deformed feldspar grain. Note that biotite are transformed into chlorite along shear zone. (c) Sigma-type asymmetric feldspar porphyroclast enclosed by dynamically recrystallized quartz grains. (d) Shear bands formed by dynamically recrystallized elongate quartz grains and smeared biotites, indicating a top-to-the-NE sense of shear. (e) Feldspar porphyroclasts exhibiting domino-type asymmetric boudins. Angle between the boudin plane and the boudin surface (Θ) is 65°. (f) Asymmetric mica fish surrounded by dynamically recrystallized quartz grains. All asymmetric structures indicate a top-to-the-NE sense of shear. q – quartz; plg – plagioclase; pf – potassium feldspar; bio – biotite; chl – chlorite. A colour version of this figure is available in online Supplementary Material at http://www.cambridge.org/journals/geo.

zones, and the textural characteristics of the Alaçamdağ granites are consistent with shallow intrusions. The depth of emplacement, however, differs relatively in the western and eastern stocks. A wider contact zone with common skarn mineralizations and occurrence of hornfelsic rocks around the equigranular western stocks suggest a relatively deeper emplacement of the western stock than the porphyritic eastern stock, which has only a centimetre-scale chilled contact zone (cf. Meinert, 1983, 1993; Misra, 2000, p. 445). Porphyritic

https://doi.org/10.1017/S0016756809990719 Published online by Cambridge University Press

Table 3. Measurements of brittle faults overprinting the mylonitized eastern stocks

Easting	Northing	Strike	Dip	Sense	Rake	Rake sense	Type	RUP (%)	α	Principal stress axes	*R*
Station: Damlıca-1											
648495	4358796	124	87	S	70	E	Normal	31	3		
648560	4358763	115	46	S	70	E	Normal	42	21		
648560	4358763	80	77	S	85	E	Normal	16	7	$\sigma_1 = 010°/69°$	
648560	4358763	51	89	S	85	W	Normal	53	20	$\sigma_2 = 274°/2°$	0.368
648560	4358763	74	84	S	79	W	Normal	25	4	$\sigma_3 = 183°/21°$	
648560	4358763	107	85	S	83	W	Normal	33	16		
648560	4358763	125	77	S	87	W	Normal	27	13		
Station: Damlıca-2											
647897	4359851	18	72	W	48	N	Normal	14	5		
647897	4359851	17	89	W	46	N	Normal	32	9		
647897	4359851	1	85	W	45	N	Normal	32	3	$\sigma_1 = 088°/71°$	
647904	4359849	5	81	W	45	N	Normal	25	0	$\sigma_2 = 233°/16°$	0.578
647904	4359849	20	75	W	55	N	Normal	13	3	$\sigma_3 = 326°/10°$	
647904	4359849	22	87	W	50	N	Normal	30	9		
647904	4359849	25	76	W	60	N	Normal	17	7		

RUP (%): values below 50% indicate good fits between actual fault slip data and computed shear distributions; α: average angle between computed shear stress and observed fault slip data (in degrees); $\sigma_{1,2,3}$: trend and plunge of the principal stress axes (in degrees); $R = (\sigma_2 - \sigma_3)/(\sigma_1 - \sigma_3)$. Easting and northing coordinates of fault locations are given in Universal Transverse Mercator (UTM) grid system. See Figure 7 for location of the stations.

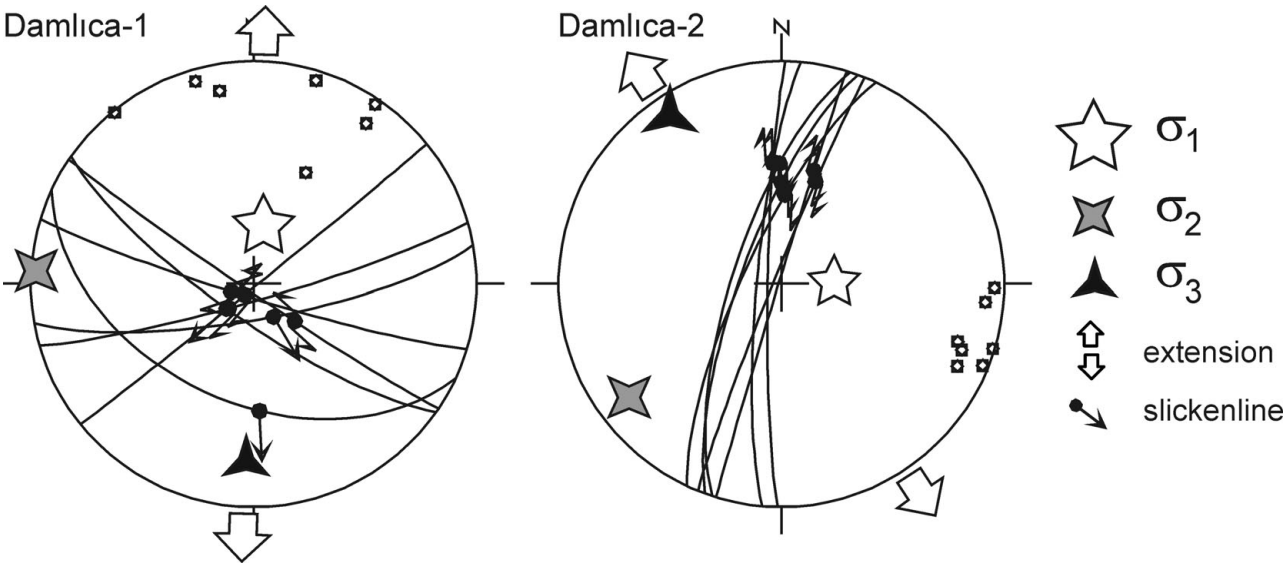

Figure 12. Schmidt lower hemisphere equal-area projections of fault-slip data and principal stress directions from the brittle faults in the eastern stocks. Refer to Table 3 for fault-slip measurements.

texture of the eastern stocks can be attributed to the textural coarsening of large K-feldspar megacrysts (cf. Coleman *et al.* 2005; Johnson, Glazner & Coleman, 2006). The Koyunoba and Eğrigöz plutons located to the east of the Alaçamdağ area are also considered as shallow-seated intrusions (Işık, Tekeli & Seyitoğlu, 2004; Ring & Collins, 2005) (Fig. 2). Radiometric age data from the Eğrigöz pluton yielded overlapping intrusion and cooling ages between *c.* 21 and 19.3 Ma, indicating rapid cooling in the order of $> 200\,^{\circ}$C/Ma and a very shallow intrusion depth (Bingöl, Delaloye & Ataman, 1982; Işık, Tekeli & Seyitoğlu, 2004; Ring & Collins, 2005). Recent U–Pb zircon dating from the Alaçamdağ granites yielded a crystallization age of 20.7 ± 1.1 Ma (Hasözbek *et al.* 2009). Although only a single crystallization age is available from the Alaçamdağ granites, Ar–Ar biotite cooling ages (20.82 to 19.51 Ma) together with U–Pb zircon ages can be correlated with the intrusion and cooling ages of the Koyunoba and Eğrigöz plutons. Hence, the Alaçamdağ granites are most likely to have cooled rapidly at very shallow depths, as supported by their field and petrographic characteristics.

The internal structure and map patterns of isolated intrusions of the Alaçamdağ granites resemble rhomb-shaped pull-apart geometries of passively emplaced plutons (Figs 4, 7). Laboratory analogue models and natural examples suggest that the shape of intrusions and pull-apart spaces or basins may give insights into the geometry of the strike-slip systems (Basile & Brun, 1999; Corti, Moratti & Sani, 2005). The length and width ratio (l_m/w_m) of an intrusion is independent of

https://doi.org/10.1017/S0016756809990719 Published online by Cambridge University Press

the scale of granite intrusions or pull-apart spaces. The constant ratio of length and width (l/w) calculated from natural and experimental examples ranges between 2.2 and 3.8, which may be slightly modified with increasing strike-slip displacement (Basile & Brun, 1999). Isolated intrusions in the Alaçamdağ area with l/w ratios of 2.2 and 2.6 define typical symmetrical rhomb-shaped spaces as recorded in the natural and laboratory examples of the strike-slip models (Table 1) (cf. Basile & Brun, 1999). Geometrical shape and l/w ratio of 1.8 measured from stock B are strikingly similar to the granitoids emplaced in a strike-slip setting (Fig. 2). Stock B of the western stocks might have occurred in a NE–SW-trending strike-slip shear zone developed by NE–SW-directed extension coupled with NW–SE-directed compressional forces, forming a reverse asymmetric geometry probably related to the low horizontal displacement of the shear zone and high emplacement rate of intrusion (cf. Corti, Moratti & Sani, 2005). When field relations of stocks are compared to results obtained from the small-scale experiments, emplacement of the Alaçamdağ granites is closely linked to the NE–SW-trending sinistral faults that formed symmetrical and asymmetrical pull-apart spaces, leading to the passive emplacement of the stocks. Passive emplacement of the western stocks is supported by lack of any magmatic foliation, which is commonly exposed in the shear-related granitoids (cf. Koukouvelas, Pe-Piper & Piper, 1996; Lacroix, Sawyer & Chown, 1998; Koukouvelas & Kokkalas, 2003).

6.b. Tectonic setting of shear zones

While the western shear zone is characterized by a moderately dipping ultramylonitic and minor mylonitic fabrics, the fabrics in the eastern shear zone are mostly gently dipping structures formed in the protomylonites and minor mylonites. Crystal-plastic processes are the dominant deformation mechanism in the shear zone rocks, as suggested by variably deformed quartz and feldspar grains. Deformation of quartz is expressed by dynamic recrystallization, subgrain formation, well-developed undulose extinction and microfracturing. Brittle deformation of quartz grains (microfractures and undulose extinction) occurs below 300 °C, while dynamic recrystallization occurs around and/or above 300 and 400 °C (Passchier & Trouw, 2005). Feldspars are deformed in a brittle manner; microfractures and domino-style asymmetric boudin structures indicate low-grade deformation at around 300–400 °C (Pryer, 1993). They are transformed into sericite in high-strain zones under retrograde conditions and show no evidence of dynamic recrystallization which begins above 400 °C (Tullis & Yund, 1985). Crystal-plastic behaviour of quartz and feldspars suggests deformation at greenschist-facies conditions, thus confirming shallow crustal levels for their deformation.

Asymmetric structures in the western and eastern shear zones consist of shear bands, sigma-type quartz and feldspar porphyroclasts, oblique-grain-shape foliation, asymmetric boudins and mica fish, and they all indicate that upper levels have moved southwestward in the western shear zone and northeastward in the eastern shear zone. The sense of shear is consistent with N–S- or NE–SW-trending crustal-scale horizontal extension. Mylonitic shear zones are overprinted by brittle faults, fractures and veins on the structurally upper parts of the Alaçamdağ granites. Brittle normal faults cut and displace mylonitic foliation and can be related to exhumation in an extensional setting. Biotites along mylonitic foliation planes and brittle faults are commonly transformed into chlorite, indicating retrogressive processes under decreasing temperature conditions. Ductile mylonitic lineations parallel to slickenlines of the brittle normal and oblique faults demonstrate that the regional N–S- or NE–SW-trending extensional forces formed contemporaneous ductile and brittle deformations at different crustal levels. As ductilely deformed lower crustal rocks are progressively uplifted by transfer zones, brittle faults overprint the ductile fabrics during progressive exhumation under the extensional tectonic regime (Hetzel *et al.* 1995*b*).

The eastern stock bears important field-based data for determining the timing of ductile deformation along the gently dipping shear zone, while the western stock has no evidence in support of syn-emplacement ductile deformation. The eastern shear zone deforms both porphyritic granites and relatively younger and cross-cutting aplitic dykes. Dykes are widely irregular, subhorizontally aligned, and lens-shaped or swarm-like bodies with irregular margins, which suggest syn-tectonic emplacement (Fig. 10d). Syn-tectonic deformation of the eastern stocks is also supported by progressive deformation (foliation) of aplitic dykes and porphyritic granites that have already cut the pre-existing foliation formed within the eastern stocks. Ar–Ar age data are consistent with syn-tectonic emplacement of the eastern stock; deformed and undeformed granites yielded biotite cooling ages ranging between 19.87 and 19.51 Ma.

6.c. Age of shear zones

The granitic rocks of the Alaçamdağ area have not previously been systematically dated. Ar–Ar analysis on biotites has been performed. Because the eastern porphyritic granites have been interpreted as synextensional, the Ar–Ar biotite ages may represent a younger limit for the ductile deformation. I therefore conclude that the age of the eastern shear zone in the Alaçamdağ area is Early Miocene (19.87–19.51 Ma). Timing of ductile deformation in the eastern shear zone is correlated with the Ar–Ar cooling age of mantle-driven mildly alkaline basalts (19.7 Ma), which are syn-sedimentary extrusions inferred to have been emplaced in a transtensional basin associated with NE–SW-trending shear zones located about 30 km to the west of the Alaçamdağ area (Erkül, Helvacı & Sözbilir, 2005*b*, 2006). Formation of detachment faults

https://doi.org/10.1017/S0016756809990719 Published online by Cambridge University Press

in the northern Menderes Massif commenced around *c*. 23 Ma, but the timing of cessation of fault activity is controversial: while some suggest *c*. 19 Ma (Thomson & Ring, 2006), others argue for younger ages (up to 15 Ma: Işık, Tekeli & Seyitoğlu, 2004). The new ages from the Alaçamdağ granites are slightly younger than previously documented ages from the mylonites of the Simav detachment (Ar–Ar muscovite and biotite ages of 22.86 Ma and 20.19 Ma: Işık & Tekeli, 2001; Işık, Tekeli & Seyitoğlu, 2004).

6.d. Origin of folding in the eastern shear zone

Structural data from the Alaçamdağ area show that the mylonitic fabric in the eastern stock is deformed along NE–SW-trending meso- to map-scale folds, which appear to be symmetrical (Fig. 7). Similar folds were recorded in the footwall rocks of extensional detachments in the Cycladic and the Menderes massifs (Bozkurt & Park, 1997*a*,*b*; Avigad, Ziv & Garfunkel, 2001; Bozkurt, 2003). Folds described in the central Menderes Massif are thought to be part of the Gediz detachment, which form a turtle-back fault surface containing mylonitic lineations on the footwall between N10°E and N30°E (Sözbilir, 2001; Çemen *et al.* 2005). Attitudes of mylonitic foliations recorded from metamorphic rocks of the central Menderes Massif closely resemble those documented from the folds in the mylonitized eastern stocks of the Alaçamdağ granites. Large-scale antiformal structures in the footwall of the Gediz detachment were attributed to the extension-perpendicular compressional forces developed during Early Miocene times (Çemen *et al.* 2006). In the Cycladic Massif, compressional structures recorded on the islands of Naxos, Paros, Tinos and Andros consist of kilometre-scale antiforms and synforms with axes parallel or slightly oblique to the NE–SW stretching lineation associated with the extensional detachments inferred to have formed during Early Miocene times (Avigad & Garfunkel, 1991). These folds are thought to be associated with coeval increments of E–W-directed horizontal shortening with approximately constant NNE–SSW stretching (Avigad, Ziv & Garfunkel, 2001).

The origin of these folds was attributed either to flow of weak lower crust material from elevated regions to extended regions (Avigad, Ziv & Garfunkel, 2001) or to the motion on the North Anatolian Fault squeezing the Aegean region between E–W-converging plates (Koçyiğit, Yusufoğlu & Bozkurt, 1999; Bozkurt, 2003; Kaya *et al.* 2004; Bozkurt & Rojay, 2005; Emre & Sözbilir, 2007). The North Anatolian Fault Zone is thought to have propagated from eastern to western Turkey since *c.* 13 to 11 Ma (Şengör *et al.* 2005; Bektaş, Eyüboğlu & Maden, 2007). In the Alaçamdağ area, field relations of folds having NE–SW-trending axes parallel to the stretching lineations along gently dipping shear zones indicate that compression is likely to accompany the crustal-scale extension during ductile deformation. The NW–SE horizontal shortening within the Early Miocene Alaçamdağ granites clearly predates the propagation of the North Anatolian Fault in western Turkey. However, a series of folds overprinting the Early–Middle Miocene sedimentary successions and reverse faults related to the approximately E–W-directed compression were also documented from western Turkey (Koçyiğit, Yusufoğlu & Bozkurt, 1999; Gökten, Havzoğlu & Şan, 2001; Bozkurt, 2003; Kaya *et al.* 2004; Bozkurt & Rojay, 2005; Erkül, Helvacı & Sözbilir, 2005*a*; Emre & Sözbilir, 2007), suggesting post-Middle Miocene activity of the compressional forces, probably associated with inception of the North Anatolian Fault. I infer that folds defined by foliation within the Alaçamdağ granites were caused by coupling between NE–SW stretching and NW–SE shortening of ductilely deformed crust during Early Miocene times. It can be claimed that a NE–SW- and NNE–SSW-directed extension was probably accompanied by compressional forces at varying degrees during the ductile to brittle deformation which has operated since Early Miocene times throughout the Aegean region.

6.e. Tectonic implications

The western margin of the Alaçamdağ granites is characterized by granitic stocks which lie along the contact, juxtaposing the metamorphic rocks of the Menderes Massif to the east and mélange rocks of the İzmir–Ankara Zone. The contact zone is mainly defined by a steeply dipping ductile shear zone between the granites and the recrystallized limestones. These contact relations suggest that the western margin of the Menderes Massif is delineated by a discrete shear zone or fault. The shear zones or faults associated with granitic intrusions in the Alaçamdağ area coincide with the eastern margin of a regional-scale shear zone, which is well exposed between Balıkesir and İzmir (Fig. 1). Recent research has enabled recognition of the NE-trending strike-slip shear zones, which are thought to be part of the regional-scale transfer zone or wrench corridor (Ring, Laws & Bernet, 1999; Sözbilir *et al.* 2003; Özkaymak & Sözbilir, 2008; Uzel & Sözbilir, 2008). The transfer zone or wrench corridor, named the İzmir–Balıkesir transfer zone, is at least 150 km long and 60 km wide, following the trend of the İzmir–Ankara Zone in the NE direction (Fig. 1) (Ring, Laws & Bernet, 1999; Özkaymak & Sözbilir, 2008; Uzel & Sözbilir, 2008). The zone separates two orogenic domains having different structural evolutions: the Sakarya Zone to the west and the Menderes Massif to the east. A number of structures exposed along the İzmir–Balıkesir transfer zone indicate the activity of the zone since Early Miocene times: (1) NE–SW-trending alignment of the Early–Middle Miocene volcanic centres coeval with continental/lacustrine deposits (Genç *et al.* 2001; Erkül, Helvacı & Sözbilir, 2005*a*,*b*; Innocenti *et al.* 2005); (2) NE–SW-trending transtensional zones represented by the Miocene pull-apart-like continental/lacustrine basins (Erkül, Helvacı & Sözbilir, 2005*b*); (3) Neogene transtensional

https://doi.org/10.1017/S0016756809990719 Published online by Cambridge University Press

supradetachment basins located between the İzmir–Ankara Zone and the Menderes Massif (Kemalpaşa–Torbalı basin: Sözbilir *et al.* 2004); (4) Plio–Quaternary basins controlled and overprinted by the NE–SW-trending strike-slip faults forming the transfer zone (Cumaovası and Manisa basins: Özkaymak & Sözbilir, 2008; Uzel & Sözbilir, 2008); and (5) NE–SW-trending clusters of earthquake epicentres with focal mechanism solutions, indicating sinistral and dextral strike-slip offsets (Özkaymak & Sözbilir, 2008; Tan, Tapırdamaz & Yörük, 2008; Uzel & Sözbilir, 2008; Akyol & Karagöz, 2009).

The onset, timing and kinematic nature of the İzmir–Balıkesir transfer zone are still subject to debate. Okay & Siyako (1993) suggested that the İzmir–Balıkesir transfer zone is a crustal-scale transform fault between the Menderes Massif and the Sakarya Zone and was a depositional site for the mélange rocks during Late Cretaceous–Paleocene collisional Tethyan orogeny. Based on the structural data from Samos Island, Ring, Laws & Bernet (1999) proposed a sinistral wrench corridor, the İzmir–Balıkesir transfer zone, that accommodated the differential extension between the severely extended Aegean and the moderately extended Menderes Massif during Miocene times. Southwestern continuation of the İzmir–Balıkesir transfer zone has already been described as the Mid-Cycladic lineament, mainly based on published palaeomagnetic data that reveal anticlockwise rotation between the Cyclades and western Turkey (Kissel & Laj, 1988; Walcott & White, 1998). The Mid-Cycladic lineament is a crustal-scale shear zone formed by an anticlockwise rotation, which has played a significant role in bringing magmas to mid-crustal levels (Walcott & White, 1998; Pe-Piper, Piper & Matarangas, 2002; Koukouvelas & Kokkalas, 2003). The lineament was responsible for the emplacement of the synextensional Naxos and Delos plutons during Middle Miocene times, according to emplacement/cooling age data of *c.* 14–12 Ma (Pe-Piper, Piper & Matarangas, 2002). The Mid-Cycladic lineament probably formed prior to *c.* 14 Ma and ceased its activity in Latest Miocene to Pliocene times, coevally with the development of the North Anatolian Fault (Walcott & White, 1998), while the İzmir–Balıkesir transfer zone was active from Early Miocene to recent times. The İzmir–Balıkesir transfer zone and the Mid-Cycladic lineament in the Aegean region are major crustal-scale shear zones, which are likely to have a close relationship during the tectonic history of the Aegean region. However, a temporal and spatial relationship between these structures remains unclear.

I propose that the NE–SW-trending shear zones are deeply extending pathways along which the magmas ascended into mid- to shallow-crustal levels in northwestern Turkey. The heat supplied by the magmas contributed to the formation of metamorphic core complexes as shown by the evidence of steep- and shallow-dipping ductile shear zones, detachment faults and synextensional magmatism. The İzmir–Balıkesir transfer zone has presumably accommodated the differential stretching between the Cycladic and Menderes massifs. It commenced *c.* 21–20 Ma and led to formation of the Kazdağ and Simav detachments in the north and Tinos, Paros and Cretan detachments in the central part of the Aegean region (Fig. 13a). The Kazdağ and Simav detachments are closely associated with synextensional granite intrusions, whereas Aegean detachments of Early Miocene age did not include granitoids intruded into the footwall rocks.

The western shear zone in the Alaçamdağ area indicates a consistent top-to-the-southwest shear sense, suggesting a sinistral offset along the transfer zone. However, the eastern shear zone is shallow dipping and indicates a top-to-the-northeast sense of shear, displaying strikingly opposite directions of hanging-wall movement than those of the western shear zone. These hanging-wall movement directions may have formed under NE–SW-directed horizontal extension, implying a spatial and temporal relationship of these shear zones consistent with regional extension of the Aegean region. These kinematic indicators also revealed that juxtaposed unmetamorphic and metamorphic rock assemblages have been sinistrally displaced along the western shear zone that accommodated the northeastward movement of the İzmir–Ankara Zone along a shallow-dipping detachment above the footwall rocks of the synextensional western stocks and the Menderes Massif during Early Miocene times. Timing of movement on the detachments located in the western and eastern parts of the transfer zone appears to be different in northwestern Turkey. Top-to-the-northeast hanging-wall movement directions in the eastern shear zone can be correlated with those recorded from the detachment-related shear zones in the Kazdağ and Simav regions (Okay & Satır, 2000; Işık & Tekeli, 2001) (Fig. 13a). Apatite fission-track data combined with sedimentary analysis from the supradetachment basins indicate that the Kazdağ detachment was active during Early to Middle Miocene times (*c.* 20–10 Ma) (Cavazza, Okay & Zattin, 2009). On the other hand, synextensional Koyunoba pluton and Alaçamdağ granites associated with the Simav detachment are unconformably overlain by felsic volcanic rocks of Early Miocene age, suggesting that the Simav detachment took place over a short time period between 24 and 19 Ma (Ring & Collins, 2005). The southern Menderes shear zone had started to develop between high-grade and the overlying low-grade metamorphic rocks in the southern Menderes Massif. Detachment faults of Early Miocene age in the northern and southern Menderes massifs mark a symmetrical extension, while extensional deformation is represented by the consistent top-to-the-northeast movement of hanging-wall related to an asymmetric extension in the Cycladic Massif. These contrasting behaviours of diverse tectonic domains in an extensional setting may have been controlled by the transfer zone activity that probably commenced in the Early Miocene (*c.* 21 Ma).

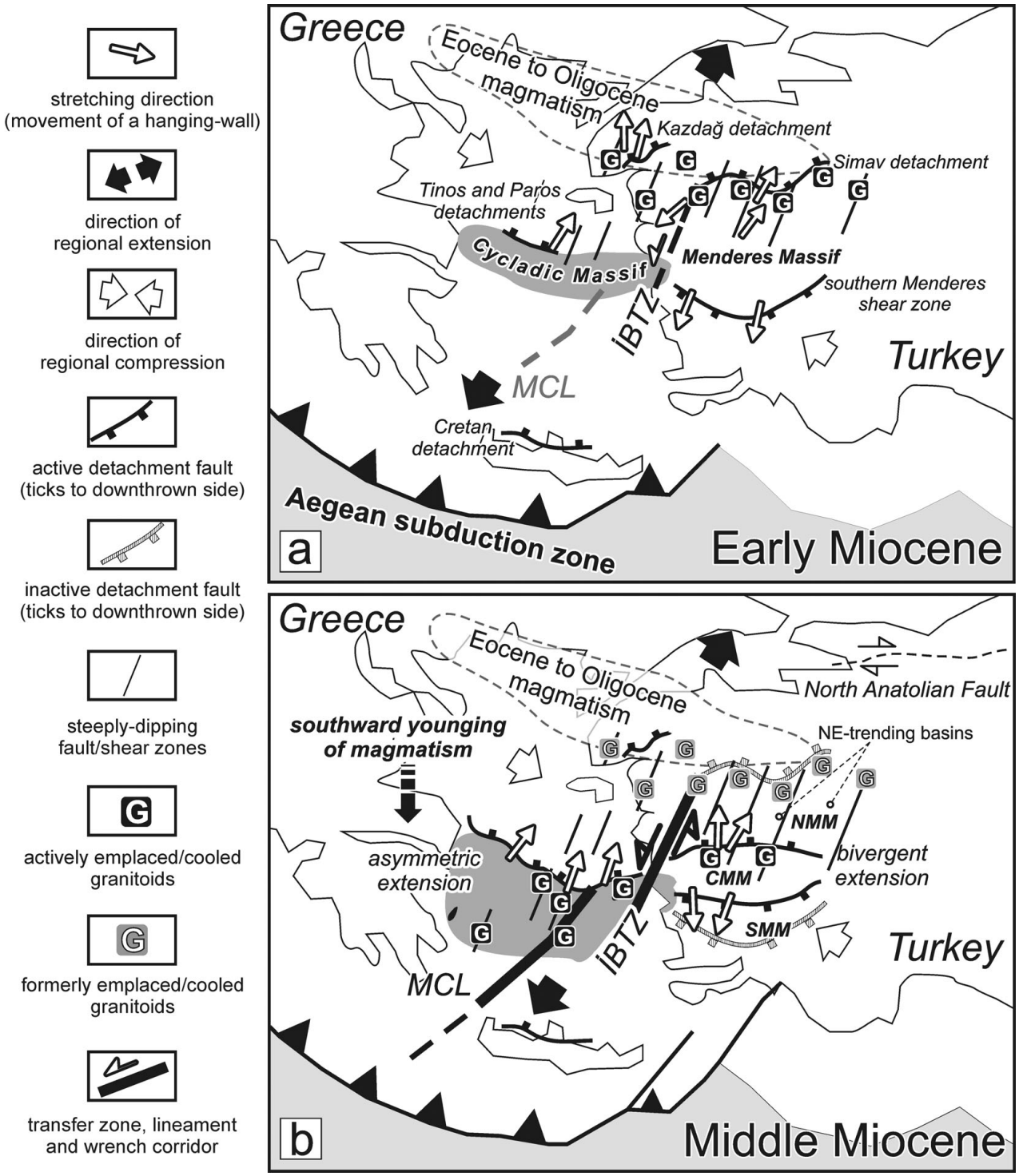

Figure 13. A schematic scenario illustrating the relationships of crustal-scale shear zones, detachment faults and syntectonic magmatic rocks in the Aegean region. (a) NE-trending shear zones with sinistral displacement started to develop under a NE–SW-trending extensional regime in Early Miocene times. Symmetrical extension occurred in the Menderes Massif, leading to the formation of metamorphic core complexes in the northwestern Turkey. North-facing detachments were active in the Aegean region, and contributed to the exhumation of the Cycladic Massif. The İzmir–Balıkesir transfer zone accommodated the differential stretching between the Aegean and western Turkey. (b) Uniform southward younging of magmatism during Early to Middle Miocene times. The İzmir–Balıkesir transfer zone and the Mid-Cycladic lineament were active during development of core complexes. Bivergent and asymmetrical extensions formed in the Menderes and Cycladic massifs, respectively. İBTZ – İzmir–Balıkesir transfer zone; MCL – Mid-Cycladic lineament; NMM – northern Menderes Massif; CMM – central Menderes Massif; SMM – southern Menderes Massif.

The activity of the İzmir–Balıkesir transfer zone continued during Middle Miocene times, leading to the bivergent and asymmetrical extensions in the Menderes and Cycladic massifs, respectively. Bivergent extension in western Turkey has been defined by the Gediz and Büyük Menderes detachments that were accompanied by the Salihli and Turgutlu granodiorites (emplacement ages of 15.0 and 16.1 Ma) intruded into the footwall

https://doi.org/10.1017/S0016756809990719 Published online by Cambridge University Press

rocks of the central Menderes Massif (Fig. 13b). North- and south-facing extensional detachments divided the Menderes Massif into three parts: northern, central and southern Menderes massifs during Middle Miocene times. Bivergent extension also formed cross-graben in the northern Menderes Massif, which have been shaped by the NE-trending basin-bounding faults feeding volcanic rocks of Early–Middle Miocene age (Şengör, 1987; Bozkurt, 2003). Episodic metamorphic core complex formation is mainly defined in the NE-trending basins that unconformably overlie the pre-existing detachment surface related to the Simav metamorphic core complex of Early Miocene age (Purvis & Robertson, 2004, 2005).

Metamorphic core-complex formation in the Cycladic Massif continued during Middle to Late Miocene times. Magmatism in the region was emplaced into the NE–SW-trending ductile shear zones and Mid-Cycladic lineament beneath the footwall of the extensional detachments. While the Cycladic Massif underwent ductile deformation, western Turkey experienced a brittle deformation that caused formation of E–W-trending horst-graben and block-fault systems coeval with the inception of the North Anatolian Fault during Late Miocene times. Brittle deformation in the central Menderes Massif is characterized by high-angle normal and oblique-slip faults that cross-cut the pre-existing Gediz detachment in the central Menderes Massif (Bozkurt & Sözbilir, 2004). Brittle deformation is also represented by occurrences of the mantle-derived basaltic rocks, which have been formed under an extensional regime without any evidence of subduction input (Yılmaz *et al.* 2001; Aldanmaz, 2002; Aldanmaz *et al.* 2006). Magmatic rocks of Early to Middle Miocene age exposed in the Aegean region have different compositions with typical geochemical subduction signatures, implying that the magmatic rocks in the Aegean and western Turkey share a common origin (Pe-Piper, Kotopouli & Piper, 1997; Altherr & Siebel, 2002; Karacık, Yılmaz & Pearce, 2007). The origin of the magmatism has been attributed to the Miocene extension and continuing subduction in a back-arc setting.

The cause of the extensional setting and formation of metamorphic core complexes in the Aegean region has been commonly explained by gravitational or orogenic collapse (Seyitoğlu & Scott, 1996) and retreat of the Aegean subduction zone (Le Pichon & Angelier, 1979, 1981; Thomson, Stöckhert & Brix, 1998). According to the orogenic collapse model, regions surrounding extensional domains are commonly subjected to radial spreading that causes radial fault systems and compressional fields toward the outer rim (Platt & Vissers, 1989). Thick crust and high potential energy for orogenic regions are required for development of the orogenic collapse, aided by plate boundary forces having a significant effect on extension (Schellart & Lister, 2004). The crustal thickness of northwestern Turkey has been inferred to be about 50 km, including voluminous magmatic input (Okay & Satır, 2000), which is not thick enough to generate convective thinning of a lithosphere. Shear zones causing extensive magmatism with uniform NE directions were predominant structures in the Aegean region during Early to Middle Miocene times. These shear zones form crustal-scale linear structures rather than radial fault systems, which can be explained by lateral slab segmentation caused by the deceleration of the NE-directed convergence between the Eurasian upper plate and the African lower plate (Kaya *et al.* 2007). A plausible mechanism appears to be the lateral slab segmentation, which was formed by increasing thickness of the African continental lower plate from west to east, leading to the sinistral oblique-slip tearing within the Eurasian upper plate (Nur & Ben-Avraham, 1978). Kinematic features of the western shear zone in the Alaçamdağ area are consistent with the proposed sinistral oblique-slip tearing defined by the regional-scale İzmir–Balıkesir transfer zone. When structural data from the Alaçamdağ area were combined with those from the adjacent metamorphic core complexes, exhumation and core complex formation were localized along the shear zones, some of which form a plate boundary between diverse tectonic units. Hence, metamorphic core complexes in the Aegean region evolved during transcurrent motion of segments due to the retreat of the Aegean subduction zone. A gravitational collapse mechanism alone is unlikely for regional extension causing development of the core complexes in the Aegean region.

Outcrop patterns of the granitic intrusions, together with volcanic centres, mark a southward younging of magmatism (Fytikas *et al.* 1984; Delaloye & Bingöl, 2000) that occurred along the NE–SW-trending shear zones, including the İzmir–Balıkesir transfer zone and the Mid-Cycladic lineament. The shear zones and magmatic rocks display a close spatial and temporal relationship and a major proportion of the Early–Middle Miocene volcanic/plutonic rocks in the central and eastern Aegean regions appear to have been emplaced along the NE–SW-trending fault zones that deformed the hanging-wall and footwall rocks of the extensional detachments. These structural features suggest that the central Aegean and western Turkey experienced subduction-related magmatism during at least Early to Middle Miocene times. Magmatism in the Aegean region formed successive and overlapping E–W-trending belts, each of which became younger more or less progressively from north to south during Eocene to Middle Miocene times. I argue that the thermal effect of magmatism contributes to the promotion of upper crustal ductile thinning and the development of core complexes (Okay & Satır, 2000; Pe-Piper, Piper & Matarangas, 2002). However, the pattern of extension appears to differ significantly in the western and eastern parts of the İzmir–Balıkesir transfer zone. Contrasting patterns of extension forming metamorphic core complexes, together with the almost uniform southward-younging magmatism, led me to suggest that a major transfer

https://doi.org/10.1017/S0016756809990719 Published online by Cambridge University Press

zone, the İzmir–Balıkesir transfer zone, accommodated the regional extension localized in upper to mid-crustal levels. Extensive magmatism was mainly controlled by the slab motion that formed a subduction-related magma brought to shallow crustal levels or to the surface by volcanic activity along deeply plunging shear zones reaching lithospheric mantle during Early Miocene times. Southward retreat of the Aegean subduction zone in the Aegean region has also been defined by younging of high-pressure metamorphism (Ring & Layer, 2003). Subduction-related magmatism forming southward-younging belts occurred in western Turkey during Early to Middle Miocene times, while subduction-related processes have been operating in the central Aegean region until recently, as marked by the active volcanic arc. Subduction-related magmatism ceased after the Middle Miocene in western Turkey, and mantle-driven basaltic volcanism has occurred in an intra-plate setting since Late Miocene to recent times, probably due to the slab detachment in western Turkey (Westaway, 2006; Agostini *et al.* 2008). These arguments could well explain the absence of subduction-related granitoids intruding the footwall of the southern Menderes shear zone and the Tinos, Paros and Cretan extensional detachments, where the subducting slab was presumably not deep enough for melt generation by subduction-related processes during Early Miocene times.

7. Conclusions

The Alaçamdağ granites consist mainly of equigranular and porphyritic granites syntectonically emplaced into the shallow crustal levels due to the development of the NE–SW-trending sinistral shear zones. These shear zones fed granitic magmas that promoted the development of metamorphic core complexes under a NE–SW extensional regime during Early Miocene times. Steep- and shallow-dipping ductile shear zones including mylonitic and ultramylonitic rocks overprinted by brittle deformation demonstrate progressive uplift and exhumation of the Alaçamdağ area under an extensional tectonic regime. Kinematic indicators from the shear zones mark hanging-wall movements of top-to-the-NE and -SW, consistent with NE–SW-trending extension in the Aegean region.

Mesoscopic- to map-scale folds in the shallow-dipping shear zones in the Alaçamdağ area were interpreted to have been caused by coupling between NE–SW stretching and the accompanying NW–SE shortening of ductilely deformed crust during Early Miocene times.

Southwest-directed displacements within the western stocks were interpreted to be associated with a regional-scale wrench corridor, that is, the İzmir–Balıkesir transfer zone. The İzmir–Balıkesir transfer zone sinistrally displaced the İzmir–Ankara Zone and the Menderes Massif, and accommodated the northeastward movement of the İzmir–Ankara Zone along an extensional detachment with footwall rocks including synextensional granites during Early–Middle Miocene times. The zone also accommodated the differential stretching between the Cycladic and the Menderes massifs, which were subjected to asymmetrical and bivergent extensions, respectively.

The NE–SW-trending shear zones and the major crustal-scale transfer zones can be explained by the combination of retreat of the Aegean subduction zone and the lateral slab segmentation due to the increasing thickness of the African continental lower plate, leading to sinistral oblique-slip tearing within the Eurasian upper plate.

Acknowledgements. This research has been supported by TÜBİTAK (Project no. 104Y274). The financial support of the scientific research project of Akdeniz University is acknowledged. The author would like to thank Sibel Tatar Erkül who helped with describing and outlining the mineralogy of the Alaçam granites. Terry Spell and Cahit Helvacı are thanked for providing Ar–Ar age data. The author is also grateful to Davut Uzuner, the Mayor of the Bigadiç district, for logistical support, and to Özgür Karaoğlu for field assistance during the fieldwork campaign. Helpful comments of Hasan Sözbilir improved the earlier version of the manuscript. The editor Mark Allen, referee Sarah J. Boulton and an anonymous referee are also thanked for their useful comments.

References

AGOSTINI, S., RYAN, J. G., TONARINI, S. & INNOCENTI, F. 2008. Drying and dying of a subducted slab: Coupled Li and B isotope variations in Western Anatolia Cenozoic Volcanism. *Earth and Planetary Science Letters* **272**, 139–47.

AKAL, C. & HELVACI, C. 1999. Mafic microgranular enclaves in the Kozak granodiorite, western Anatolia. *Turkish Journal of Earth Sciences* **8**, 1–17.

AKDENİZ, N. & KONAK, N. 1979. *The geology of Simav, Emet, Dursunbey and Demirci regions*. Ankara, Turkey: General Directorate of Mineral Research and Exploration (MTA) Report no. 6547 (in Turkish).

AKYOL, N. & KARAGÖZ, Ö. 2009. Empirical attenuation relationships for Western Anatolia, Turkey. *Turkish Journal of Earth Sciences* **18**, 351–82.

ALDANMAZ, E. 2002. Mantle source characteristics of alkali basalts and basanites in an extensional intracontinental plate setting, Western Anatolia, Turkey: Implications for multi-stage melting. *International Geology Review* **44**, 440–57.

ALDANMAZ, E., PEARCE, J. A., THIRLWALL, M. F. & MITCHELL, J. G. 2000. Petrogenetic evolution of Late Cenozoic, post-collision volcanism in western Anatolia, Turkey. *Journal of Volcanology and Geothermal Research* **102**, 67–95.

ALDANMAZ, E., KÖPRÜBAŞI, N., GÜRER, Ö. F., KAYMAKÇI, N. & GOURGAUD, A. 2006. Geochemical constraints on the Cenozoic, OIB-type alkaline volcanic rocks of NW Turkey: Implications for mantle sources and melting processes. *Lithos* **86**, 50–76.

ALTHERR, R. & SIEBEL, W. 2002. I-type plutonism in a continental back-arc setting: Miocene granitoids and monzonites from the central Aegean Sea, Greece. *Contributions to Mineralogy and Petrology* **143**, 397–415.

ALTUNKAYNAK, Ş. & YILMAZ, Y. 1998. The Mount Kozak magmatic complex, Western Anatolia. *Journal of Volcanology and Geothermal Research* **85**, 211–31.

ALTUNKAYNAK, Ş. & YILMAZ, Y. 1999. The Kozak Pluton and its emplacement. *Geological Journal* **34**, 257–74.

ANGELIER, J. 1984. Tectonic stress analysis of fault slip data sets. *Journal of Geophysical Research* **89**, 5835–48.

ANGELIER, J. 1989. From orientation to magnitudes in paleostress determinations using fault slip data. *Journal of Structural Geology* **11**, 37–50.

ANGELIER, J. 1990. Inversion of field data in fault tectonics to obtain regional stress. III. A new rapid direct inversion method by analytical means. *Geophysical Journal International* **103**, 363–76.

AVIGAD, D. & GARFUNKEL, Z. 1991. Uplift and exhumation of high-pressure metamorphic terrains: the example of the cycladic blueschist belt (Aegean Sea). *Tectonophysics* **188**, 357–72.

AVIGAD, D., BAER, G. & HEIMANN, A. 1998. Block rotations and continental extension in the central Aegean Sea: palaeomagnetic and structural evidence from Tinos and Mykonos (Cyclades, Greece). *Earth and Planetary Science Letters* **157**, 23–40.

AVIGAD, D., ZIV, A. & GARFUNKEL, Z. 2001. Ductile and brittle shortening, extension-parallel folds and maintenance of crustal thickness in the central Aegean (Cyclades, Greece). *Tectonics* **20**, 277–87.

AYDOĞAN, M. S., ÇOBAN, H., BOZCU, M. & AKINCI, Ö. 2008. Geochemical and mantle-like isotopic (Nd, Sr) composition of the Baklan Granite from the Muratdağı Region (Banaz, Uşak), western Turkey: Implications for input of juvenile magmas in the source domains of western Anatolia Eocene–Miocene granites. *Journal of Asian Earth Sciences* **33**, 155–76.

BASILE, C. & BRUN, J. P. 1999. Transtensional faulting patterns ranging from pull-apart basins to transform continental margins: an experimental investigation. *Journal of Structural Geology* **21**, 23–37.

BECCALETTO, L., BARTOLINI, A. C., MARTINI, R., HOCHULI, P. A. & KOZUR, H. 2005. Biostratigraphic data from the Çetmi Mélange, northwest Turkey: Palaeogeographic and tectonic implications. *Palaeogeography Palaeoclimatology Palaeoecology* **221**, 215–44.

BEKTAŞ, O., EYÜBOĞLU, Y. & MADEN, N. 2007. Different modes of stress transfer in a strike-slip fault zone: an example from the North Anatolian Fault System in Turkey. *Turkish Journal of Earth Sciences* **16**, 1–12.

BESTMANN, M., PRIOR, D. J. & VELTKAMP, K. T. A. 2004. Development of single-crystal σ-shaped quartz porphyroclasts by dissolution–precipitation creep in a calcite marble shear zone. *Journal of Structural Geology* **26**, 869–83.

BİNGÖL, E., DELALOYE, M. & ATAMAN, G. 1982. Granitic intrusions in western Anatolia: a contribution to the geodynamic study of this area. *Eclogae Geologicae Helvetiae* **75**, 437–46.

BOZKURT, E. 2001. Late Alpine evolution of the central Menderes Massif, western Anatolia, Turkey. *International Journal of Earth Sciences* **89**, 728–44.

BOZKURT, E. 2003. Origin of NE-trending basins in western Turkey. *Geodinamica Acta* **16**, 61–81.

BOZKURT, E. 2004. Granitoid rocks of the southern Menderes Massif (southwestern Turkey): field evidence for Tertiary magmatism in an extensional shear zone. *International Journal of Earth Sciences* **93**, 52–71.

BOZKURT, E. & PARK, R. G. 1994. Southern Menderes Massif – an incipient metamorphic core complex in western Anatolia, Turkey. *Journal of the Geological Society, London* **151**, 213–16.

BOZKURT, E. & PARK, R. G. 1997*a*. Microstructures of deformed grains in the augen gneisses of southern Menderes Massif (western Turkey) and their tectonic significance. *Geologische Rundschau* **86**, 103–19.

BOZKURT, E. & PARK, R. G. 1997*b*. Evolution of a mid-Tertiary extensional shear zone in the southern Menderes massif, western Turkey. *Bulletin de la Société Géologique de France* **168**, 3–14.

BOZKURT, E. & PARK, R. G. 1999. The structure of the Palaeozoic schists in the southern Menderes Massif, western Turkey: a new approach to the origin of the main Menderes Metamorphism and its relation to the Lycian Nappes. *Geodinamica Acta* **12**, 25–42.

BOZKURT, E. & SATIR, M. 2000. The southern Menderes Massif (western Turkey): geochronology and exhumation history. *Geological Journal* **35**, 285–96.

BOZKURT, E. & OBERHÄNSLI, R. 2001. Menderes Massif (Western Turkey): structural, metamorphic and magmatic evolution – a synthesis. *International Journal of Earth Sciences* **89**, 679–708.

BOZKURT, E. & SÖZBİLİR, H. 2004. Tectonic evolution of the Gediz Graben: field evidence for an episodic, two-stage extension in western Turkey. *Geological Magazine* **141**, 63–79.

BOZKURT, E. & ROJAY, B. 2005. Episodic, two-stage Neogene extension and short-term intervening compression in Western Turkey: field evidence from the Kiraz Basin and Bozdağ Horst. *Geodinamica Acta* **18**, 299–316.

BOZTUĞ, D., HARLAVAN, Y., JONCKHEERE, R., CAN, İ. & SARI, R. 2009. Geochemistry and K–Ar cooling ages of the Ilıca, Çataldağ (Balıkesir) and Kozak (İzmir) granitoids, west Anatolia, Turkey. *Geological Journal* **44**, 79–103.

BRÖCKER, M. & FRANZ, L. 1998. Rb–Sr isotope studies on Tinos Island (Cyclades, Greece); additional time constraints for metamorphism, extent of infiltration-controlled overprinting and deformational activity. *Geological Magazine* **135**, 369–82.

BUICK, I. S. 1991. The late Alpine evolution of an extensional shear zone, Naxos, Greece. *Journal of the Geological Society, London* **148**, 93–103.

CANDAN, O., DORA, O. Ö., OBERHÄNSLI, R., ÇETİNKAPLAN, M., PARTZSCH, J. H., WARKUS, F. C. & DÜRR, S. 2001. Pan-African high-pressure metamorphism in the Precambrian basement of the Menderes Massif, western Anatolia, Turkey. *International Journal of Earth Sciences* **89**, 793–811.

CAVAZZA, W., OKAY, A. & ZATTIN, M. 2009. Rapid Early–Middle Miocene exhumation of the Kazdağ Massif (western Anatolia). *International Journal of Earth Sciences* **98**, 1935–47.

COLEMAN, D. S., BARTLEY, J. M., GLAZNER, A. F. & LAW, R. D. 2005. Incremental assembly and emplacement of Mesozoic plutons in the Sierra Nevada and White and Inyo Ranges, California. *Geological Society of America Field Forum Field Trip Guide* (Rethinking the Assembly and Evolution of Plutons: Field Tests and Perspectives, 7–14 October 2005), 59 pp., doi:10.1130/2005.MCBFYT.FFG.

CORTI, G., MORATTI, G. & SANI, F. 2005. Relations between surface faulting and granite intrusions in analogue models of strike-slip deformation. *Journal of Structural Geology* **27**, 1547–62.

ÇEMEN, İ., TEKELİ, O., SEYİTOĞLU, G. & IŞIK, V. 2005. Are turtleback fault surfaces common structural elements

of highly extended terranes? *Earth-Science Reviews* **73**, 139–48.

ÇEMEN, İ., CATLOS, E. J., GÖĞÜŞ, O. & ÖZERDEM, C. 2006. Postcollisional extensional tectonics and exhumation of the Menderes massif in the Western Anatolia extended terrane, Turkey. In *Postcollisional Tectonics and Magmatism in the Mediterranean Region and Asia* (ed. Y. Dilek), pp. 353–79. Geological Society of America Special Publication.

DELALOYE, M. & BİNGÖL, E. 2000. Granitoids from Western and Northwestern Anatolia: Geochemistry and modeling of geodynamic evolution. *International Geology Review* **42**, 241–68.

DELVAUX, D., MOEYS, R., STAPEL, G., MELNIKOV, A. & ERMIKOV, V. 1995. Palaeostress reconstructions and geodynamics of the Baikal region, Central Asia, Part I. Palaeozoic and Mesozoic pre-rift evolution. *Tectonophysics* **252**, 61–101.

DEWEY, J. F. 1988. Extensional collapse of orogens. *Tectonics* **7**, 1123–39.

DİLEK, Y. & ALTUNKAYNAK, Ş. 2007. Cenozoic crustal evolution and mantle dynamics of post-collisional magmatism in western Anatolia. *International Geology Review* **49**, 431–53.

DOGLIONI, C., AGOSTINI, S., CRESPI, M., INNOCENTI, F., MANETTI, P., RIGUZZI, F. & SAVAŞÇIN, Y. 2002. On the extension in Western Anatolia and the Aegean sea. In *Reconstruction of the Evolution of the Alpine–Himalayan Orogen* (eds G. Rosenbaum & G. S. Lister), pp. 169–84. Journal of the Virtual Explorer.

DURU, M., PEHLİVAN, S., ŞENTÜRK, Y., YAVAŞ, F. & KAR, H. 2004. New results on the lithostratigraphy of the Kazdağ Massif in northwest Turkey. *Turkish Journal of Earth Sciences* **13**, 177–86.

EMRE, T. & SÖZBİLİR, H. 2007. Tectonic evolution of the Kiraz Basin, Küçük Menderes Graben: Evidence for compression/uplift-related basin formation overprinted by extensional tectonics in West Anatolia. *Turkish Journal of Earth Sciences* **16**, 441–70.

ERDOĞAN, B. & GÜNGÖR, T. 2004. The problem of the core-cover boundary of the Menderes Massif and an emplacement mechanism for regionally extensive gneissic granites, western Anatolia (Turkey). *Turkish Journal of Earth Sciences* **13**, 15–36.

ERKÜL, F., HELVACI, C. & SÖZBİLİR, H. 2005*a*. Evidence for two episodes of volcanism in the Bigadiç borate basin and tectonic implications for western Turkey. *Geological Journal* **40**, 545–70.

ERKÜL, F., HELVACI, C. & SÖZBİLİR, H. 2005*b*. Stratigraphy and geochronology of the Early Miocene volcanic units in the Bigadiç borate basin, Western Turkey. *Turkish Journal of Earth Sciences* **14**, 227–53.

ERKÜL, F., HELVACI, C. & SÖZBİLİR, H. 2006. Olivine basalt and trachyandesite peperites formed at the subsurface/surface interface of a semi-arid lake: An example from the Early Miocene Bigadiç basin, western Turkey. *Journal of Volcanology and Geothermal Research* **149**, 240–62.

FORSTER, M. A. & LISTER, G. S. 1999. Detachment faults in the Aegean Core Complex of Ios, Greece. In *Exhumation processes: normal faulting, ductile flow and erosion* (eds U. Ring, M. T. Brandon, G. S. Lister & S. D. Willett), pp. 305–23. Geological Society of London, Special Publication no. 154.

FOSTER, D. A. & FANNING, C. M. 1997. Geochronology of the northern Idaho batholith and the Bitterroot metamorphic core complex: Magmatism preceding and contemporaneous with extension. *Geological Society of America Bulletin* **109**, 379–94.

FOSTER, D. A., SCHAFER, C., FANNING, C. M. & HYNDMAN, D. W. 2001. Relationships between crustal partial melting, plutonism, orogeny, and exhumation: Idaho-Bitterroot batholith. *Tectonophysics* **342**, 313–50.

FYTIKAS, M., INNOCENTI, F., MANETTI, P., MAZZUOLI, R., PECCERILLO, A. & VILLARI, L. 1984. Tertiary to Quaternary evolution of volcanism in the Aegean region. In *The Geological evolution of the Eastern Mediterranean* (eds J. E. Dixon & A. H. F. Robertson), pp. 687–99. Geological Society of London, Special Publication no. 17.

FYTIKAS, M., GIULIANI, O., INNOCENTI, F., MANETTI, P., MAZZUOLI, R., PECCERILLO, A. & VILLARI, L. 1979. Neogene Volcanism of the Northern and Central Aegean region. *Annales Géologiques des Pays Helléniques* **30**, 106–29.

GAUTIER, P. & BRUN, J. P. 1994. Ductile crust exhumation and extensional detachments in the central Aegean (Cyclades and Evia Islands). *Geodinamica Acta* **7**, 57–85.

GENÇ, S. C. 1998. Evolution of the Bayramiç magmatic complex, northwestern Anatolia. *Journal of Volcanology and Geothermal Research* **85**, 233–49.

GENÇ, S. C., ALTUNKAYNAK, Ş., KARACIK, Z., YAZMAN, M. & YILMAZ, Y. 2001. The Çubukludağ graben, south of İzmir: its tectonic significance in the Neogene geological evolution of the western Anatolia. *Geodinamica Acta* **14**, 45–55.

GESSNER, K., PIAZOLO, S., GÜNGÖR, T., RING, U., KRONER, A. & PASSCHIER, C. W. 2001*a*. Tectonic significance of deformation patterns in granitoid rocks of the Menderes nappes, Anatolide belt, southwest Turkey. *International Journal of Earth Sciences* **89**, 766–80.

GESSNER, K., RING, U., JOHNSON, C., HETZEL, R., PASSCHIER, C. W. & GÜNGÖR, T. 2001*b*. An active bivergent rolling-hinge detachment system; central Menderes metamorphic core complex in western Turkey. *Geology* **29**, 611–14.

GLODNY, J. & HETZEL, R. 2007. Precise U–Pb ages of syn-extensional Miocene intrusions in the central Menderes Massif, western Turkey. *Geological Magazine* **144**, 235–46.

GOSCOMBE, B. D. & PASSCHIER, C. N. 2003. Asymmetric boudins as shear sense indicators – an assessment from field data. *Journal of Structural Geology* **25**, 575–89.

GÖKTEN, E., HAVZOĞLU, T. & ŞAN, O. 2001. Tertiary evolution of the central Menderes Massif based on structural investigations of metamorphics and sedimentary cover rocks between Salihli and Kiraz (western Turkey). *International Journal of Earth Sciences* **89**, 745–56.

HASÖZBEK, A., SATIR, M., ERDOĞAN, B., AKAY, E. & SIEBEL, W. 2009. U–Pb geochronology and Sr–Nd isotopic composition of collision related granites in NW Anatolia: contrasting petrogenetic evolution of the magmatic suites. In *62th Geological Kurultai of Turkey Abstract Book* (ed. Anonymous), pp. 490–1. Ankara, Turkey: Chamber of Geological Engineering of Turkey.

HEJL, E., RIEDL, H. & WEINGARTNER, H. 2002. Post-plutonic unroofing and morphogenesis of the Attic–Cycladic complex (Aegea, Greece). *Tectonophysics* **349**, 37–56.

HETZEL, R., PASSCHIER, C. W., RING, U. & DORA, O. Ö. 1995*a*. Bivergent Extension in Orogenic Belts: the Menderes Massif (Southwestern Turkey). *Geology* **23**, 455–8.

HETZEL, R., RING, U., AKAL, C. & TROESCH, M. 1995*b*. Miocene NNE-directed extensional unroofing in the

Menderes Massif, southwestern Turkey. *Journal of the Geological Society, London* **152**, 639–54.

HETZEL, R., ROMER, R. L., CANDAN, O. & PASCHIER, C. W. 1998. Geology of the Bozdağ area, central Menderes massif, SW Turkey: Pan-African basement and Alpine deformation. *Geologische Rundschau* **87**, 394–406.

HİSARLI, Z. M. & DOLMAZ, M. N. 2004. Kozak plütonik kütlesinin havadan magnetik anomalilerinin modellenmesi. *İstanbul Üniversitesi Mühendislik Fakültesi Yerbilimleri Dergisi* **17**, 147–59.

INNOCENTI, F., AGOSTINI, S., DI VINCENZO, G., DOGLIONI, C., MANETTI, P., SAVAŞCIN, M. Y. & TONARINI, S. 2005. Neogene and Quaternary volcanism in Western Anatolia: Magma sources and geodynamic evolution. *Marine Geology* **221**, 397–421.

IŞIK, V. & TEKELİ, O. 2001. Late orogenic crustal extension in the northern Menderes Massif (western Turkey); evidence for metamorphic core complex formation. In *Menderes Massif (western Turkey): structural, metamorphic and magmatic evolution* (eds E. Bozkurt & R. Oberhänsli), pp. 757–65. Berlin: Springer International.

IŞIK, V., TEKELİ, O. & SEYİTOĞLU, G. 2004. The $^{40}Ar/^{39}Ar$ age of extensional ductile deformation and granitoid intrusion in the northern Menderes core complex: implications for the initiation of extensional tectonics in western Turkey. *Journal of Asian Earth Sciences* **23**, 555–66.

JOHNSON, B. R., GLAZNER, A. F. & COLEMAN, D. S. 2006. Potassium feldspar megacrysts in granites: passive markers of magma dynamics or products of textural coarsening? *EOS Transactions of the American Geophysical Union* **87**(52), Fall Meeting Supplement, Abstract V51B-1670.

JOLIVET, L. 2001. A comparison of geodetic and finite strain pattern in the Aegean, geodynamic implications. *Earth and Planetary Science Letters* **187**, 95–104.

JOLIVET, L. & BRUN, J.-P. In press. Cenozoic geodynamic evolution of the Aegean. *International Journal of Earth Sciences*, doi:10.1007/s00531–008-0366-4.

JOLIVET, L., RIMMELE, G., OBERHÄNSLI, R., GOFFE, B. & CANDAN, O. 2004. Correlation of syn-orogenic tectonic and metamorphic events in the Cyclades, the Lycian nappes and the Menderes massif. Geodynamic implications. *Bulletin de la Société Géologique de France* **175**, 217–38.

JUSTET, L. & SPELL, T. L. 2001. Effusive eruptions from a large silicic magma chamber: the Bearhead Rhyolite, Jemez volcanic field, NM. *Journal of Volcanology and Geothermal Research* **107**, 241–64.

KARACIK, Z. & YILMAZ, Y. 1998. Geology of the ignimbrites and the associated volcano-plutonic complex of the Ezine area, northwestern Anatolia. *Journal of Volcanology and Geothermal Research* **85**, 251–64.

KARACIK, Z., YILMAZ, Y. & PEARCE, J. A. 2007. The Dikili-Çandarlı volcanics, Western Turkey: magmatic interactions as recorded by petrographic and geochemical features. *Turkish Journal of Earth Sciences* **16**, 493–522.

KAYA, O., ÜNAY, E., GÖKTAŞ, F. & SARAÇ, G. 2007. Early Miocene stratigraphy of central west Anatolia, Turkey: implications for the tectonic evolution of the eastern Aegean area. *Geological Journal* **42**, 85–109.

KAYA, O., ÜNAY, E., SARAÇ, G., EICHHORN, S., HASSENRUCK, S., KNAPPE, A., PEKDEĞER, A. & MAYDA, S. 2004. Halitpaşa transpressive zone: Implications for an Early Pliocene compressional phase in central western Anatolia, Turkey. *Turkish Journal of Earth Sciences* **13**, 1–13.

KISSEL, C. & LAJ, C. 1988. The Tertiary geodynamical evolution of the Aegean arc: a paleomagnetic reconstruction. *Tectonophysics* **146**, 183–201.

KOÇYİĞİT, A., YUSUFOĞLU, H. & BOZKURT, E. 1999. Evidence from the Gediz graben for episodic two-stage extension in western Turkey. *Journal of the Geological Society, London* **156**, 605–16.

KORALAY, O. E., DORA, O. Ö., CHEN, F., SATIR, M. & CANDAN, O. 2004. Geochemistry and geochronology of orthogneisses in the Derbent (Alaşehir) area, eastern part of the Ödemiş-Kiraz submassif, Menderes Massif: Pan-African magmatic activity. *Turkish Journal of Earth Sciences* **13**, 37–61.

KOUKOUVELAS, I., PE-PIPER, G. & PIPER, D. J. W. 1996. Pluton emplacement by wall-rock thrusting, hanging-wall translation and extensional collapse: Latest Devonian plutons of the Cobequid fault zone, Nova Scotia, Canada. *Geological Magazine* **133**, 285–98.

KOUKOUVELAS, I. K. & KOKKALAS, S. 2003. Emplacement of the Miocene west Naxos pluton (Aegean Sea, Greece): a structural study. *Geological Magazine* **140**, 45–61.

LACROIX, S., SAWYER, E. & CHOWN, E. 1998. Pluton emplacement within an extensional transfer zone during dextral strike-slip faulting: an example from the Late Archaean Abitibi Greenstone Belt. *Journal of Structural Geology* **20**, 43–59.

LE PICHON, X. & ANGELIER, J. 1979. The Aegean arc and trench system: a key to the neotectonic evolution of the Eastern Mediterranean area. *Tectonophysics* **60**, 1–42.

LE PICHON, X. & ANGELIER, J. 1981. The Aegean Sea. *Philosophical Transactions of the Royal Society of London Series A – Mathematical Physical and Engineering Sciences* **300**, 357–72.

LE PICHON, X., BERGERAT, F. & ROULET, M. J. 1988. Plate kinematics and tectonics leading to Alpine belt formation: a new analysis. In *Processes in Continental Lithospheric Deformation* (eds S. P. Clark, B. C. Burchfiel & J. Suppe), pp. 111–31. Geological Society of America Special Papers.

LE PICHON, X., LALLEMANT, S. J., CHAMOT-ROOKE, N., LEMEUR, D. & PASCAL, G. 2002. The Mediterranean Ridge backstop and the Hellenic nappes. *Marine Geology* **186**, 111–25.

LEE, J. & LISTER, G. S. 1992. Late Miocene ductile extension and detachment faulting, Mykonos, Greece. *Geology* **20**, 121–4.

LIPS, A. L. W., CASSARD, D., SÖZBİLİR, H., YILMAZ, H. & WIJBRANS, J. R. 2001. Multistage exhumation of the Menderes Massif, western Anatolia (Turkey). *International Journal of Earth Sciences* **89**, 781–92.

LISTER, G. S. & BALDWIN, S. L. 1993. Plutonism and the origin of metamorphic core complexes. *Geology* **21**, 607–10.

MEINERT, L. D. 1983. Variability of skarn deposits-Guides to exploration. In *Revolution in the Earth Sciences* (ed. S. J. Boardman), pp. 301–16. Kendall-Hunt Dubuque, SA.

MEINERT, L. D. 1993. Igneous petrogenesis and skarn deposits. In *Mineral Deposit Modeling* (eds R. V. Kirkham, W. D. Sinclair, R. I. Thorpe & J. M. Duke), pp. 569–83. Geological Society of Canada, Special Paper no. 40.

MEULENKAMP, J. E., WORTEL, M. J. R., VAN WAMEL, W. A., SPAKMAN, W. & HOOGERDUYN STRATING, E. 1988. On the Hellenic subduction zone and the geodynamic evolution of Crete since the late Middle Miocene. *Tectonophysics* **146**, 203–15.

MISRA, K. C. 2000. *Understanding mineral deposits*. Dordrecht: Kluwer Academic Publishers, 845 pp.

NUR, A. & BEN-AVRAHAM, Z. 1978. The eastern Mediterranean and the Levant: Tectonics of continental collision. *Tectonophysics* **46**, 297–312.

OBERHÄNSLI, R., MONIE, P., CANDAN, O., WARKUS, F. C., PARTZSCH, J. H. & DORA, O. O. 1998. The age of blueschist metamorphism in the Mesozoic cover series of the Menderes Massif. *Schweizerische Mineralogische und Petrographische Mitteilungen* **78**, 309–16.

OKAY, A. İ. 2001. Stratigraphic and metamorphic inversions in the central Menderes Massif; a new structural model. *International Journal of Earth Sciences* **89**(4), 709–27.

OKAY, A. İ. & SİYAKO, M. 1993. The revised location of the İzmir–Ankara Suture in the region between Balıkesir and İzmir (In Turkish). In *Tectonics and Hydrocarbon Potential of Anatolia and Surrounding Regions* (ed. S. Turgut), pp. 333–55. Turkish Association of Petroleum Geologists, Ankara.

OKAY, A. İ. & SATIR, M. 2000. Coeval plutonism and metamorphism in a Latest Oligocene metamorphic core complex in northwest Turkey. *Geological Magazine* **137**, 495–516.

OKAY, A. İ. & ALTINER, D. 2007. A condensed Mesozoic succession north of İzmir: A fragment of the Anatolide–Tauride platform in the Bornova Flysch zone. *Turkish Journal of Earth Sciences* **16**, 257–79.

ÖZGENÇ, İ. & İLBEYLİ, N. 2008. Petrogenesis of the Late Cenozoic Eğrigöz pluton in western Anatolia, Turkey: Implications for magma genesis and crustal processes. *International Geology Review* **50**, 375–91.

ÖZKAYMAK, C. & SÖZBİLİR, H. 2008. Stratigraphic and structural evidence for fault reactivation: The active Manisa fault zone, western Anatolia. *Turkish Journal of Earth Sciences* **17**, 615–35.

PASSCHIER, C. & COELHO, S. 2006. An outline of shear-sense analysis in high-grade rocks. *Gondwana Research* **10**, 66–76.

PASSCHIER, C. N. & TROUW, R. A. J. 2005. *Microtectonics, 2nd ed.* Berlin: Springer-Verlag, 289 pp.

PE-PIPER, G. 2000. Origin of S-type granites coeval with I-type granites in the Hellenic subduction system, Miocene of Naxos, Greece. *European Journal of Mineralogy* **12**, 859–75.

PE-PIPER, G., KOTOPOULI, C. N. & PIPER, D. J. W. 1997. Granitoid rocks of Naxos, Greece: regional geology and petrology. *Geological Journal* **32**, 153–71.

PE-PIPER, G., PIPER, D. J. W. & MATARANGAS, D. 2002. Regional implications of geochemistry and style of emplacement of Miocene I-type diorite and granite, Delos, Cyclades, Greece. *Lithos* **60**, 47–66.

PLATT, J. & VISSERS, R. 1989. Extensional collapse of thickened continental lithosphere: a working hypothesis for the Alboran Sea and the Gibraltar arc. *Geology* **17**, 540–3.

PRYER, L. L. 1993. Microstructures in feldspars from a major crustal thrust zone: The Grenville Front, Ontario, Canada. *Journal of Structural Geology* **15**, 21–36.

PURVIS, M. & ROBERTSON, A. 2004. A pulsed extension model for the Neogene–Recent E–W-trending Alaşehir Graben and the NE–SW-trending Selendi and Gördes Basins, western Turkey. *Tectonophysics* **391**, 171–201.

PURVIS, M. & ROBERTSON, A. 2005. Miocene sedimentary evolution of the NE–SW-trending Selendi and Gördes basins, W Turkey: Implications for extensional processes. *Sedimentary Geology* **174**, 31–62.

RIMMELÉ, G., JOLIVET, L., OBERHÄNSLI, R. & GOFFE, B. 2003*a*. Deformation history of the high-pressure Lycian Nappes and implications for tectonic evolution of SW Turkey. *Tectonics* **22**, 1–21.

RIMMELÉ, G., OBERHÄNSLI, R., GOFFE, B., JOLIVET, L., CANDAN, O. & ÇETİNKAPLAN, M. 2003*b*. First evidence of high-pressure metamorphism in the "Cover Series" of the southern Menderes Massif. Tectonic and metamorphic implications for the evolution of SW Turkey. *Lithos* **71**, 19–46.

RING, U. & LAYER, P. W. 2003. High-pressure metamorphism in the Aegean, eastern Mediterranean: Underplating and exhumation from the Late Cretaceous until the Miocene to Recent above the retreating Hellenic subduction zone. *Tectonics* **22**(3), 1022, doi:10.1029/2001TC001350, 22 pp.

RING, U. & COLLINS, A. S. 2005. U–Pb SIMS dating of synkinematic granites: timing of core-complex formation in the northern Anatolide belt of western Turkey. *Journal of the Geological Society, London* **162**, 289–98.

RING, U. & KUMERICS, C. 2008. Vertical ductile thinning and its contribution to the exhumation of high-pressure rocks: the Cycladic blueschist unit in the Aegean. *Journal of the Geological Society, London* **165**, 1019–30.

RING, U., LAWS, S. & BERNET, M. 1999. Structural analysis of a complex nappe sequence and late-orogenic basins from the Aegean Island of Samos, Greece. *Journal of Structural Geology* **21**, 1575–1601.

RING, U., THOMSON, S. N. & BRÖCKER, M. 2003. Fast extension but little exhumation: the Vari detachment in the Cyclades, Greece. *Geological Magazine* **140**, 245–52.

RING, U., JOHNSON, C., HETZEL, R. & GESSNER, K. 2003. Tectonic denudation of a Late Cretaceous–Tertiary collisional belt: regionally symmetric cooling patterns and their relation to extensional faults in the Anatolide belt of western Turkey. *Geological Magazine* **140**, 421–41.

RING, U., WILL, T., GLODNY, J., KUMERICS, C., GESSNER, K., THOMSON, S., GÜNGÖR, T., MONIE, P., OKRUSCH, M. & DRUPPEL, K. 2007. Early exhumation of high-pressure rocks in extrusion wedges: Cycladic blueschist unit in the eastern Aegean, Greece, and Turkey. *Tectonics* **26**, TC2001, doi:10.1029/2005TC001872.

SANCHEZ-GOMEZ, M., AVIGAD, D. & HEIMANN, A. 2002. Geochronology of clasts in allochthonous Miocene sedimentary sequences on Mykonos and Paros Islands: implications for back-arc extension in the Aegean Sea. *Journal of the Geological Society, London* **159**, 45–60.

SCHELLART, W. & LISTER, G. 2004. Tectonic models for the formation of arc-shaped cenvergent zones and back-arc basins. *Geological Society of America Special Paper* **383**, 237–58.

SCHUILING, R. D. 1962. Türkiye'nin güneybatısındaki Menderes migmatit kompleksinin petrolojisi, yaşı ve yapısı hakkında. *Maden Tetkik Arama Enstitüsü Dergisi* **58**, 70–85.

SEYİTOĞLU, G. & SCOTT, B. C. 1996. The cause of N–S extensional tectonics in western Turkey: Tectonic escape vs back-arc spreading vs orogenic collapse. *Journal of Geodynamics* **22**, 145–53.

SEYİTOĞLU, G., IŞIK, V. & ÇEMEN, İ. 2004. Complete Tertiary exhumation history of the Menderes massif, western Turkey: an alternative working hypothesis. *Terra Nova* **16**, 358–64.

SÖZBİLİR, H. 2001. Extensional tectonics and the geometry of related macroscopic structures with their relations to the extensional tectonics: Field evidence from the Gediz

detachment, western Turkey. *Turkish Journal of Earth Sciences* **10**, 51–67.

SÖZBİLİR, H. 2002. Geometry and origin of folding in the Neogene sediments of the Gediz Graben, western Anatolia, Turkey. *Geodinamica Acta* **15**, 277–88.

SÖZBİLİR, H., İNCİ, U., ERKÜL, F. & SÜMER, Ö. 2003. An active intermittent transform zone accommodating N–S extension in western Anatolia and its relation to the North Anatolian Fault System. In *International Workshop on the North Anatolian, East Anatolian and Dead Sea Fault Systems Abstracts*, p. 87. Middle East Technical University, Cultural Convention Center Ankara, Turkey.

SÖZBİLİR, H., SARI, B., AKGÜN, F., GÖKÇEN, N., AKKİRAZ, S., SÜMER, Ö. & ERKÜL, F. 2004. First example of a transtensional supradetachment basin in western Anatolia: the Kemalpaşa–Torbalı basin, Turkey. *32nd International Geological Congress* **1**, 173.

SPAKMAN, W., WORTEL, M. J. R. & VLAAR, N. J. 1988. The Hellenic subduction zone: a tomographic image and its geodynamic implications. *Geophysical Research Letters* **15**, 60–3.

SPELL, T. L. & MCDOUGALL, I. 2003. Characterization and calibration of $^{40}Ar/^{39}Ar$ dating standards. *Chemical Geology* **198**, 189–211.

STRECKEISEN, A. 1976. To each plutonic rock its proper name. *Earth Science Reviews* **12**, 1–33.

ŞENGÖR, A. M. C. 1984. Timing of tectonic events in the Menderes massif, Western Turkey: implications for tectonic evolution and evidence for Pan-African basement in Turkey. *Tectonics* **3**, 693–707.

ŞENGÖR, A. M. C. 1987. Cross-faults and differential stretching of hanging walls in regions of low-angle normal faulting: examples from western Turkey. In *Continental Extensional Tectonics* (eds M. P. Coward, J. F. Dewey & P. Hancock), pp. 575–89. Geological Society of London, Special Publication no. 28.

ŞENGÖR, A. M. C., SATIR, M. & AKKÖK, R. 1984. Timing of tectonic events in Menderes Massif, western Turkey. Implications for tectonic evolution and evidence for Pan-African basement in Turkey. *Tectonics* **3**, 693–707.

ŞENGÖR, A. M. C., GÖRÜR, N. & ŞAROĞLU, F. 1985. Strike-slip deformation, basin formation and sedimentation: Strike-slip faulting and related basin formation in zones of tectonic escape: Turkey as a case study. *Society of Economic Palaeontologists and Mineralogists Special Publication* **37**, 227–64.

ŞENGÖR, A. M. C., TÜYSÜZ, O., İMREN, C., SAKINÇ, M., EYİDOĞAN, H., GÖRÜR, G., LE PICHON, X. & RANGIN, C. 2005. The North Anatolian Fault: A new look. *Annual Review of Earth and Planetary Sciences* **33**, 37–112.

TAN, O., TAPIRDAMAZ, M. C. & YÖRÜK, A. 2008. The earthquake catalogues for Turkey. *Turkish Journal of Earth Sciences* **17**, 405–18.

THOMSON, S. N. & RING, U. 2006. Thermochronologic evaluation of postcollision extension in the Anatolide orogen, western Turkey. *Tectonics* **25**, TC3005, doi:10.1029/2005TC001833.

THOMSON, S. N., STÖCKHERT, B. & BRIX, M. R. 1998. Thermochronology of the high-pressure metamorphic rocks of Crete, Greece: Implications for the speed of tectonic processes. *Geology* **26**, 259–62.

THOMSON, S. N., STÖCKHERT, B. & BRIX, M. A. 1999. Miocene high-pressure metamorphic rocks of Crete, Greece: Rapid exhumation by buoyant escape. In *Exhumation processes: Normal faulting, ductile flow and erosion* (eds U. Ring, M. T. Brandon, G. S. Lister & S. D. Willett), pp. 87–108. Geological Society of London, Special Publication no. 154.

TIREL, C., GUEYDAN, F., TIBERI, C. & BRUN, J. P. 2004. Aegean crustal thickness inferred from gravity inversion. Geodynamical implications. *Earth and Planetary Science Letters* **228**, 267–80.

TRANOS, M. D., KACHEV, V. N. & MOUNTRAKIS, D. M. 2008. Transtensional origin of the NE–SW Simitli basin along the Strouma (Strymon) Lineament, SW Bulgaria. *Journal of the Geological Society, London* **165**, 499–510.

TULLIS, J. & YUND, R. A. 1982. Grain growth kinetics of quartz and calcite aggregates. *Journal of Geology* **90**, 301–18.

TULLIS, J. & YUND, R. A. 1985. Dynamic recrystallization of feldspar: A mechanism for ductile shear zone formation. *Geology* **13**, 238–41.

UZEL, B. & SÖZBİLİR, H. 2008. A first record of a strike-slip basin in western Anatolia and its tectonic implication: the Cumaovası basin. *Turkish Journal of Earth Sciences* **17**, 559–91.

VAN HINSBERGEN, D. J. J., HAFKENSCHEID, E., SPAKMAN, W., MEULENKAMP, J. E. & WORTEL, R. 2005. Nappe stacking resulting from subduction of oceanic and continental lithosphere below Greece. *Geology* **33**, 325–8.

VERGE, N. J. 1993. The exhumation of the Menderes Massif metamorphic core complex of Western Anatolia. *Terra Abstracts* **5**, 249.

WALCOTT, C. R. & WHITE, S. H. 1998. Constraints on the kinematics of post-orogenic extension imposed by stretching lineations in the Aegean region. *Tectonophysics* **298**, 155–75.

WESTAWAY, R. 2006. Cenozoic cooling histories in the Menderes Massif western Turkey, may be caused by erosion and flat subduction, not low-angle normal faulting. *Tectonophysics* **412**, 1–25.

WHITNEY, D. L. & BOZKURT, E. 2002. Metamorphic history of the southern Menderes massif, western Turkey. *Geological Society of America Bulletin* **114**, 829–38.

WHITNEY, D. L., TEYSSIER, C., KRUCKENBERG, S. C., MORGAN, V. L. & IREDALE, L. J. 2008. High-pressure–low-temperature metamorphism of metasedimentary rocks, southern Menderes Massif, western Turkey. *Lithos* **101**, 218–32.

YILMAZ, H. 2007. Stream sediment geochemical exploration for gold in the Kazdağ dome in the Biga Peninsula, western Turkey. *Turkish Journal of Earth Sciences* **16**, 33–55.

YILMAZ, Y., GENÇ, Ş. C., KARACIK, Z. & ALTUNKAYNAK, Ş. 2001. Two contrasting magmatic associations of NW Anatolia and their tectonic significance. *Journal of Geodynamics* **31**, 243–71.

YÜCEL-ÖZTÜRK, Y., HELVACI, C. & SATIR, M. 2005. Genetic relations between skarn mineralization and petrogenesis of the Evciler granitoid, Kazdağ, Çanakkale, Turkey and comparison with world skarn granitoids. *Turkish Journal of Earth Sciences* **14**, 255–80.